REFRIGERANT FORCED-CONVECTION CONDENSATION INSIDE HORIZONTAL TUBES

Soonhoon Bae

John S. Maulbetsch

Warren M. Rohsenow

Report No. DSR 79760-59

Contract No. ASHRAE RP63

Department of Mechanical Engineering
Engineering Projects Laboratory
Massachusetts Institute of Technology

November 1, 1968

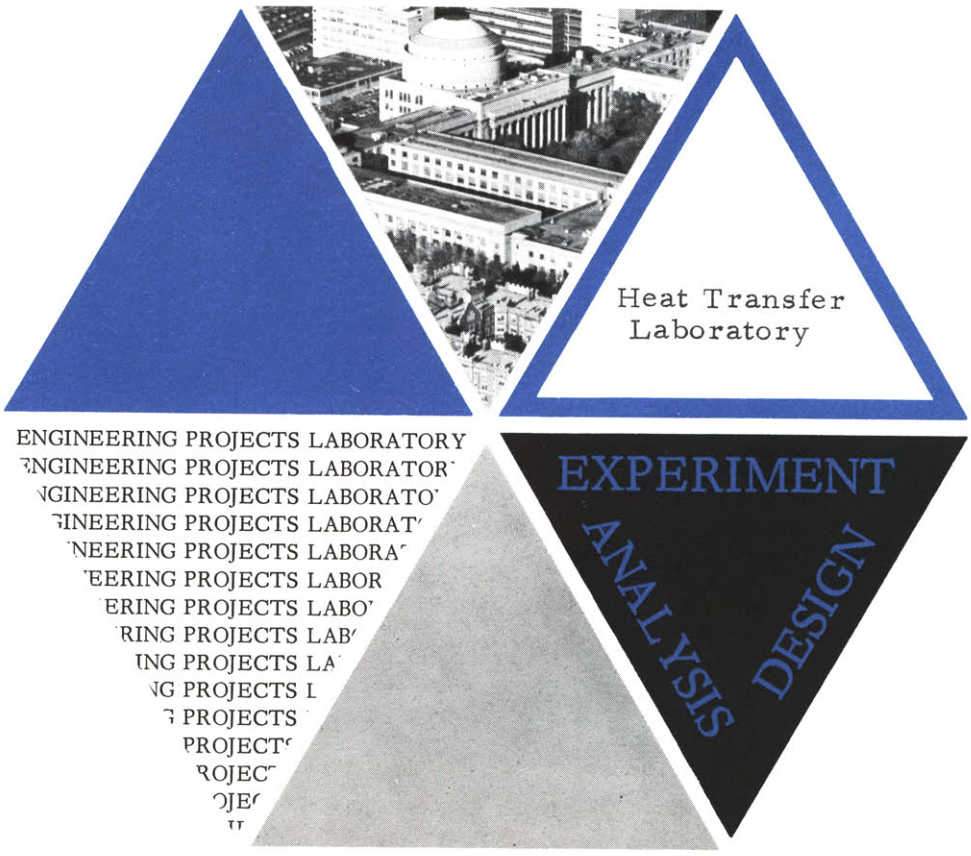

TECHNICAL REPORT NO. 79760-59

REFRIGERANT FORCED-CONVECTION CONDENSATION INSIDE HORIZONTAL TUBES

by

Soonhoon Bae
John S. Maulbetsch
Warren M. Rohsenow
Massachusetts Institute of Technology

Sponsored by:-

TECHNICAL COMMITTEE 1.3

AMERICAN SOCIETY OF HEATING, REFRIGERATING AND AIR CONDITIONING ENGINEERS

Contract No: ASHRAE RP63

DSR Project NO: 79760

November 1,1968

Heat Transfer Laboratory
Mechanical Engineering Department
Massachusetts Institute of Technology
Massachusetts Avenue, Cambridge, 02139.

REFRIGERANT FORCED-CONVECTION CONDENSATION INSIDE HORIZONTAL TUBES

by

Soonhoon Bae
John S. Maulbetsch
Warren M. Rohsenow

Massachusetts Insitute of Technology.

ABSTRACT

Condensing heat transfer rates inside a horizontal tube were investigated for large quality changes across the tube.

The proposed correlation is a modification of the work of Rohsenow, Webber and Ling [29]. The result of the investigation is modified through new variables which include the effect of the true axial pressure gradient in a tube.

Experimental data are presented for a range of flow conditions. A 0.493 in. ID, 19.75 ft. long nickel tube was used for condensing Refrigerant-12. The saturation temperature was varied from 84.6°F to 118°F and flow rates of vapor-liquid mixture ranged from 151,000 lbm/ft^2hr to 555,000 lbm/ft^2hr. The inlet quality was essentially 100% at saturation and exit qualities ranged from 50% to zero and subcooled liquid. The test results for average heat transfer coefficient were correlated by the analysis within 15%.

NOMENCLATURE

A	Cross section area	ft^2
c_p	Specific heat	Btu/lbm °F
D	Tube inner diameter	ft
D_o	Tube outer diameter	ft
f	Friction factor	
F_o	Pressure Gradient in the Tube	$lbf/ft^2/ft$
g	Gravity	ft/sec^2
G_ℓ	Mass velocity of the liquid	$lbm/hr\ ft^2$
G_v	Mass velocity of the vapor	$lbm/hr\ ft^2$
h_{fg}	Latent heat of the evaporation	Btu/lbm
h_z	Local heat transfer coefficient	$Btu/hr\ ft^2°F$
k	Conductivity of the liquid	Btu/hr ft °F
L	Length of the cooling water jacket	ft
Nu	Nusselt Number	
Pr	Prandtl Number	
(q/A)	Heat flux	Btu/ft^2hr
Re	Reynolds Number	
T_i	Inner wall temperature	°F
T_o	Outer wall temperature	°F
ΔT	Temperature difference between vapor and condensing wall	°F
ΔT	Cooling water temperature rise	°F
V_z	Velocity of the condensate flow	ft/sec
W	Flow rate of the fluid	lbm/hr
W_w	Flow rate of the cooling water	lbm/hr
z	Distance from condensation starting point	ft

Γ	Condensate flow rate per unit perimeter	lbm/hr/ft
δ	Thickness of the condensate layer	ft
σ	Surface tension of Refrigerant	lbf/ft
σ_w	Surface tension of water	lbf/ft
τ	Shear stress in the liquid layer	lbf/ft^2
τ_v	Interfacial shear stress	lbf/ft^2
μ	Viscosity of the liquid	lbm/ft hr
ν	Kinematic viscosity	ft^2/hr
ρ_ℓ	Density of the liquid	lbm/ft^3
ρ_v	Density of the vapor	lbm/ft^3

$$\lambda = \left[\left(\frac{\rho_v}{0.075}\right)\left(\frac{\rho_\ell}{62.3}\right)\right]^{\frac{1}{2}}$$

$$\psi = \frac{73}{\sigma}\left[\mu_\ell \left(\frac{62.3}{\rho_\ell}\right)^2\right]^{\frac{1}{3}}$$

INTRODUCTION

Condensation inside a horizontal tube is often encountered in a wide variety of vapor-compression refrigeration systems such as evaporation condensers, air-cooled condensers and some water-cooled condensers of the tube-in-tube type. An accurate knowledge of heat transfer coefficients and associated pressure gradients is required for the proper design of such equipment.

Most previous test work for forced convection condensing inside of horizontal tubes has been done with shorter cooled sections and small changes in quality across the test section [1], [2], [8], [10], [14] and [26]. In the present tests a long test section was used and heat transfer coefficients measured in six sections along the length. The inlet condition was essentially saturated dry vapor and the exit quality varied from 50% down to zero, and in some cases the exit was actually subcooled liquid. Condensing along the entire length more closely approximates actual operating conditions in condensers.

Since, when vapor condenses on a cold surface, the rate of condensation depends on the amount of condensate accumulated on the surface, the fluid mechanics of the condensate flow must be considered as an integral part of the heat transfer problem.

Gravity is the predominant force which removes condensate from a condensing surface. However, for the turbulent flow of condensate inside a horizontal tube, or for a zero gravity condition such as space vehicle condensers, the force due to friction at the vapor-liquid interface and momentum change of condensate flow have considerable

effect on the fluid mechanics and heat transfer rate of the flow. Therefore, the proper approach to this problem is to investigate these forces to provide a complete description of fluid flow and to use these results as input to the energy equation.

When two phases flow together in a pipe, they can arrange themselves into a variety of geometric configurations characterized by such terms as bubbly flow, slug flow, annular flow, mist flow, stratified flow and so on. It is hardly expected to find a single correlation which will apply equally well to all flow regimes. It seemed reasonable to start an analysis of an ideal flow model and to extend it to other flow regime. Since annular flow is the predominant flow regime in practice, initial models will be developed for annualar flow as in many previous works.

REVIEW OF PREVIOUS WORK

Starting from the classical Nusselt analysis [28], a considerable amount of research has been directed toward condensation phenomena. In the early stages, the general approach to this problem was equating the shear stress in the condensate flow to the gravity force and relating the increasing rate of condensate flow to the heat transfer rate. The heat transfer rate was reduced to a heat transfer coefficient with the assumption of a linear temperature distribution in the condensate layer. The assumption was proved to be a good approximation by Rohsenow's [27] complete analysis.

Tape and Mueller [32] carried out experiments to investigate the effect of flow rate, angle of inclination of the condenser-tube and temperature difference on the rate of condensation of benzene and methanol vapor. In these experiments, a 0.745 in. ID by 0.875 in. OD copper tube, jacketed over a length of 35.7 in. with a 1-inch ID copper tube, was used as a test section. Most of the empirical data were considerably higher than the corresponding calculated coefficients by Nusselt's analysis for an inclined tube. White [34] obtained data on condensation of saturated Refrigerant-12 on a plain horizontal tube at various vapor temperatures and film temperature drops. For the ideal condition of Nusselt's analysis, his experimental data, however, fall 13% below the values predicted by the Nusselt equation.

For very low condensate flow rate, Chaddock [12] redid the Nusselt analysis for a particular flow model. Chato [13] and Chen [15], using the same model of the flow, considered the momentum change of the condensate and vapor flows. The momentum and energy equation of the

film condensation problem were solved simultaneously for the condensate forming on the wall and for bottom condensate flow inside horizontal and inclined tubes. It was shown that Nusselt's analysis yields accurate results for fluids with Prandtl Numbers of the order of one or greater.

For turbulent condensate flow, Carpenter and Colburn [11] analysed the shear stress in the condensate layer taking into account the effects of gravity, momentum change and friction at the vapor-liquid interface. They hypothesized that in the presence of a high frictional force from the vapor on its outer surface, the condensate layer would become turbulent at much lower values of Reynolds Number than found when vapor friction was negligible. They also reasoned that when the major force acting on the condensate layer was vapor friction rather than gravity, the velocity distribution might follow that found for a pipe filled with liquid. The main thermal resistance in turbulent condensation heat transfer was assumed to occur in the laminar sublayer of condensate. Using von Karman's universal velocity distribution in a smooth pipe [28] and a linear temperature distribution in the laminar sublayer, they arrived at the following expression for the local heat transfer coefficient:-

$$h_z = C \left(\frac{c_p \mu}{k}\right)^{\frac{1}{2}} \frac{k \left(\rho_\ell F\right)^{\frac{1}{2}}}{\mu} \qquad (1)$$

where C is an arbitrary constant and F_o is shear force in the laminar sublayer. The shear force F_o included the effect of gravity, momentum change and friction and was determined separately by semi-empirical correlations. Experimental data were obtained by condensing pure vapors of water, methanol, toluene and trichlorethylene at high velocities inside a vertical tube 0.459 in. ID and 8 ft. long. The data scattered badly on a $\frac{h_z \mu}{k \rho^2} Pr^{-\frac{1}{2}}$ versus $F_o^{\frac{1}{2}}$ graph and also yield much higher values than those predicted by the modified Nusselt relation, which includes the effect of vapor friction on the thickness of the viscous condensate layer.

The effect of vapor shear stress was re-evaluated by Rohsenow, Webber and Ling [29] by modifying the Nusselt analysis to include the vapor shear stress. Also the effect of vapor shear stress on transition to turbulence was proposed. In this analysis the vapor shear stress was determined from air-water two-phase flow measurements and the effect of momentum changes were neglected. The analytical predictions for average heat transfer coefficient agreed well with the data of Carpenter and Colburn [11] and suggested that Eq. (1) was valid only in a limited Prandtl number range, $2 \lesssim Pr \lesssim 4$ and over a limited range of vapor shear stress values.

Altman, Staub and Norris [3] used the same method as was used in Reference [11] to correlate the data for local heat transfer coefficients for Refrigerant-22 condensing inside an 8 ft. long, 0.343 in. ID horizontal tube. The pressure gradients were correlated by the Martinelli-Nelson method [24]. Further, the turbulent portion of the condensate layer (i.e. the buffer layer) was included in the calculation

of the thermal resistance in addition to the laminar sublayer. They also proposed a correction factor for superheated vapor:-

$$\beta = 0.29\ (\Delta T)^{0.52}_{\text{superheat}} \qquad (2)$$

where β is the ratio of observed heat transfer coefficient to that predicted when neglecting the effect of superheat. Although this correction correlated the data quite well, it has no claim to general applicability.

Dukler [18] studied the problem again using the universal velocity distribution in the vertical liquid film. The differential equations for shear stress and heat transfer in the liquid film were solved numerically with a computer introducing the equation of Deissler for eddy viscosity and eddy thermal conductivity near a solid boundary. As the film thickness increases turbulence appears in the film as predicted from the universal velocity distribution and no other criterion for transition to turbulence is necessary.

Recently, Soliman, Schuster and Berenson [31] modified the Carpenter-Colburn method of evaluating the shear stress in the condensate layer. Using an annular flow model to develop a momentum equation, they redefined the shear stress due to friction, gravity and momentum change. An equation for predicting pressure drops due to interfacial vapor-shear was derived by the use of the Lockhart-Martinelli method [20] of calculating pressure gradients of isothermal two-phase, two-component flow in pipes. Zivi's equation [35] of local void fraction for annular flow was introduced for evaluating

the momentum change. However, a knowledge of the vapor quality change along the tube is required to get the momentum change. In the paper only the case of uniform heat removal along the tube was shown. Although the flow problem was more thoroughly dealt with than before, the heat transfer coefficients were calculated by Equation (1) with a changed exponent on the Prandtl Number and a new empirical constant. A consideration of the mechanics of the condensate flow indicates that the Carpenter-Colburn method, as explained in Reference [3], has some limitations. Only the thermal resistance of the laminar sublayer was considered, which should result in greater than experimental heat transfer coefficients at the lower vapor qualities. Failure to include the buffer layer between the laminar layer and turbulent vapor core should result in less than experimental heat transfer coefficients at high vapor qualities. The resulting equation (1) has two drawbacks:-

1. It does not reduce to the classical Nusselt relationship at zero vapor shear stress at the interface.
2. There is no explicit Reynolds Number effect. That is, at a constant F_o, increasing film Reynolds Numbers should lead to higher heat transfer rates.

Equation (1) is adopted in Reference [3] and [11] with the same inherent drawbacks.

Many correlations of non-dimensional type with empirically determined coefficients and exponents have been proposed. Akers, Deans and Crosser [1] correlated their data by a single-phase flow equation [28] as follows:-

$$Nu\ Pr^{-m} = C\ Re^{n} \qquad (3)$$

where all fluid properties were those of condensate evaluated at the average film temperature, and the Reynolds Number was based on an equivalent liquid mass velocity of the mixture of vapor and liquid. The empirical data was obtained for propane and Refrigerant-12 inside a 4.7ft. horizontal section of 3/4 in. galvanized pipe. Akers and Rosson [2] took data for methanol and Refrigerant-12 condensing inside a 1 ft. long horizontal tube. The data were also correlated with dimensionless groups as follows:-

For $\frac{DG}{\mu_\ell} < 5{,}000$

$$1{,}000 < \frac{DG_v}{\mu}\left(\frac{\rho_\ell}{\rho_v}\right)^{\frac{1}{2}} < 20{,}000; \quad \frac{h_z D}{k} = 1.38\left(\frac{c_p \mu}{k}\right)^{\frac{1}{3}}\left(\frac{h_{fg}}{c_p \Delta T}\right)^{\frac{1}{6}}\left[\frac{DG_v}{\mu}\left(\frac{\rho_\ell}{\rho_v}\right)^{\frac{1}{2}}\right]^{0.2} \tag{4}$$

$$20{,}000 < \frac{DG}{\mu}\left(\frac{\rho_\ell}{\rho_v}\right)^{\frac{1}{2}} < 100{,}000; \quad \frac{h_z D}{k} = 0.1\left(\frac{c_p \mu}{k}\right)^{\frac{1}{3}}\left(\frac{h_{fg}}{c_p \Delta T}\right)^{\frac{1}{6}}\left[\frac{DG_v}{\mu}\left(\frac{\rho_\ell}{\rho_v}\right)^{\frac{1}{2}}\right]^{2/3} \tag{5}$$

For: $\frac{DG_v}{\mu} < 5{,}000 \qquad \frac{DG_v}{\mu}\left(\frac{\rho_\ell}{\rho_v}\right)^{\frac{1}{2}} < 20{,}000$

$$\frac{h_z D}{k} = 0.026\left(\frac{c_p \mu}{k}\right)^{\frac{1}{3}}\left(\frac{DG_E}{\mu}\right)^{0.8} \tag{6}$$

where: $G_E = G_v\left(\frac{\rho_\ell}{\rho_v}\right)^{\frac{1}{2}} + G_\ell$

The above equations are suggested in ASHRAE Handbook of Fundamentals [6]

Chen [14] and Brauser [10] analysed the liquid film as a boundary layer and got similar non-dimensional type equation which included a Nusselt Number, Reynolds Number, Prandtl Number and Thermal Potential' ($h_{fg}/c_p\Delta T$). Those four terms seemed to permit a description of the system in terms of the heat transfer rate (Nu), the dynamic effects of

the vapor on the liquid film (Re_{ν}), the thermal properties of the liquid film (Pr) and the thermal potential ($h_{fg}/c_p\Delta T$). However, as may be seen in Figs 6&7, the scatter of the data is considerable. Furthermore, a brief physical argument indicates that a vapor Reynolds Number is not sufficient to correlate the data.

Consider two separate local conditions as an example:

I	II
$G_1 = 1.0 \times 10$ lbm/hr ft^2	$G_2 = 2.0 \times 10$ lbm/hr ft^2
$X_1 = 0.80$	$X_2 = 0.40$
$G_{\nu 1} = 0.80 \times 10$ lbm/hr ft^2	$G_{\nu 2} = 0.80 \times 10$ lbm/hr ft^2

Hence, the vapor Reynolds Number are the same. But,

$G_{\nu_1} = 0.20 \times 10$ lbm/hr ft^2	$G_{\nu 2} = 1.20 \times 10$ lbm/hr ft^2

Since primary resistance to heat transfer is associated with the liquid film, one would expect:

$$h_1 > h_2$$

Hilding and Coogan [20] added the mean thickness of the annular liquid layer to the above variables in non-dimensional manner and correlated their data for condensing steam vapor. Their final correlation indicates that the tube diameter and vapor velocities play a stronger role in determining the rate of heat transfer than does the mean thickness of the annular liquid layer.

Two Russian papers by Boyko and Kruzhilin [5,9] present a very simple

equation on the basis of an analogy between heat transfer and hydraulic resistance as follows:-

$$h_z = \frac{k}{D} (0.021)\ Re_\ell^{0.8}\ \ Pr_\ell^{0.43}\ \left(\frac{Pr_f}{Pr_w}\right)_\ell^{0.25}\ \ \left(\frac{\rho_\ell}{\rho_m}\right)^{\frac{1}{2}} \qquad (7)$$

where:

$$\frac{\rho_\ell}{\rho_m} = 1 + \frac{\rho_\ell - \rho_\nu}{\rho_\nu}\ x \qquad (8)$$

and subscripts f and w denote that the value in question is evaluated at the temperature of the stream and of the wall respectively. The REynolds Number is based on the total flow rate, liquid properties, and the tube diameter.

TEST FACILITY

General Description

The experimental apparatus was designed to provide good data over the range of parameters which would cover conditions typically encountered in the refrigeration industry. A schematic diagram of the experimental equipment is shown in Figure 1.

The basic apparatus consists of a closed-loop refrigerant flow circuit driven by a mechanical seal rotor pump. Upstream of the test section, an electrical heated boiler produces vapor, which passes through a flow-meter and a throttle valve to the test sections. Downstream of the test section, an after-condenser was provided to ensure fully condensed refrigerant at the pump inlet. The speed of the pump could be controlled by varying the supply voltage, but, in test runs, the power supply was fixed and the flow rate and pressure level of the test section was controlled by making use of a by-pass loop.

The test section itself is an annular shaped heat exchanger with refrigerant flowing through the inner tube and cooling water running in the outer annulus counter-currently in six directions. Initially, an 18 foot long, 0.493 inch ID nickel tube was used as the condensing surface and the thickness of the tube wall was determined so as to simulate the tangential variations of wall temperature and conduction heat transfer rate through the wall encountered in practice. The test section was divided into six short sections of 3 foot length.

Each short section has a separate cooling water circuit and those sections are connected with a small transparent section to permit observation of the flow regime.

Thermocouples were provided to measure the wall temperature at the middle of every short section and one of the short sections has three thermocouple junctions, spaced circumferentially, to investigate tangential variation in the wall temperature. The bulk temperature of refrigerant vapor is measured by six thermocouples located along the axial positions. The flow rate and the temperature rise of cooling water was measured across each single section. Pressure taps were installed at the inlet and outlet of every short section for measurement of pressure change.

Since the outer tube of the annulus in the test section was made of plexi-glass of 1/4 inch thickness and the water temperature was near the room temperature, the test section was not insulated. "Blank" runs were made to determine the heat losses. The maximum possible error at extreme conditions is of the order of 1% and typically of the order of 0.2%. Hence no correction was made in the data reduction. By using the heat load of the after-condenser and of the test section the heat balance was checked.

Details and Design Profedure of Apparatus

The ranges of parameters which would cover conditions typically encountered in practice are given below:

1.	Refrigerant	Ref-12 and Ref-22
2.	Tube Diameter	0.2 - 0.8 in. ID
3.	Mass Velocity	60,000 - 600,000 lbm/ft^2hr
4.	Condensing Temperature	T_{sat} = 80 - 150°F
	(P_{sat} = 100 - 250 psia for Ref-12)	
5.	Inlet Condition	0 - 150°F superheat
6.	Exit Condition	0 - 25°F subcooling
7.	Condensing Temperature Difference	(T_{vapor} - T_{wall}) 3 - 20°F

Test Section

Initially, the 3/8 - L type copper tube which is of quite common use in industry was chosen as a test section. However, wall temperature drop measurements with such a high conductivity material are extremely difficult and inaccurate. Nickel was selected for its lower conductivity. The thickness of the tube was determined so that a simulation-variable $k\delta$, a measure of the peripheral conduction, was approximately the same in the nickel and copper tubes. This was intended to simulate the tangential variations of wall temperature and heat flux of the original copper tube. The exact size of the nickel test section for the initial experiments is as follows:

Inner Diameter	0.493 inch
Outer Diameter	0.675 inch
Wall thickness	0.091 inch
Length	19.75 ft.

In later tests other tube diameters will be used.

Thermocouples are located as follows: one at the center of the tube; and one at the outside of the tube wall as shown in Figure 2.

A set of such thermocouples is placed every 3 feet along the axis at the 90° point on the side of the tube. The third 3 ft. section has two more thermocouples, one at the top and one at the bottom of the tube, to determine the tangential variation of wall temperature. The thermocouples are made of 36 gage copper-constantan wire, and the thermocouple beads were made with a Dynatech TIG Welder. Pressure taps are also attached at every 3 feet along the axis. Mercury manometers were installed to measure local pressure drops along the test section but gave erroneous readings due to condensation in the lines. This will be corrected in future tests. The absolute pressure of the system was measured at the vapor generator by a pressure gauge and verified by a saturation temperature measurement. They agreed within the precision of the pressure gauge, which corresponded to about 1.5 F.

Cooling Water Jacket

Water flows in counterflow through the outer annulus of each test section; hence as the water temperature increases in the upstream vapor direction, the wall temperature in the section tends to remain uniform. The water temperature rise through the annulus should be optimized for two contradictory conditions; small enough to neglect the wall temperature change in the axial direction and big enough to measure with precision. Each of the six sections of the water jacket is 3 feet long, and the outside of the annulus is made of a plexi-glass tube. Cooling water is supplied separately to each section. The design condition in

the cooling water jacket is as follows:

Water velocity	3 - 5 ft. per second
Pressure drop	Less than 20 psia
Temperature rise between inlet and outlet	1 - 3°F

The actual dimensions and shape of the annulus are shown in Figure 2. Water temperature rise is measured with differential thermocouples, copper-constantan.

Transparent Section

Transparent sections are provided between every short section for observation of flow regime. Material for the sections should have physical and chemical properties such that they will not be dissolved by Refrigerant 12 or 22 and have enough strength to contain the high vapor pressures (max. 400 psia). Though it is attacked slightly by Refrigerant-22, Plexi-glass was used because it is easy to machine

After-Condenser

A shell-and-tube York Standard Condenser-Receiver is used for complete condensation and subcooling after the test section. The capacity was chosen for 60% of the vapor generator capacity (40,000 Btu/hr).

Pump

Initially, a Flexi-liner pump, which has a flexible liner between the liquid passage and an eccentric shaft, was used in order to prevent oil contamination of the Refrigerant. However, the usual flexible liner, made of neoprene, is easily broken by the high system pressure.

A mechanical, sealed-rotor pump, Blackmer X51$\frac{1}{4}$ A CMax-flow rate 12 GPM, was substituted for it. Care was taken to prevent vibration of the rotor. A by-pass loop was provided for controlling the flow rate and the pressure level of the system.

Boiler

An electric resistance-heating unit was set up in a 20 in. diameter, 2 ft. long cylinder. The liquid level is always kept above the heating element to prevent burnout of the element. Maximum capacity of the heating unit is 15 Kw. Moisture content was checked visually at the transparent section of the test section. Between the boiler and the test section a throttle valve is provided for controlling the flow rate and the inlet quality of vapor.

ANALYSIS

In a paper originally published in 1956, Rohsenow, Webber and Ling [29] dealt with the effect of vapor shear stress on condensing heat transfer rates on vertical surfaces. The classical Nusselt analysis was modified (see Figure 3) through the inclusion of an interfacial shear stress term as:-

$$-g_o\tau = \frac{\mu dV_z}{dy} = g(\rho_\ell - \rho_v)(\delta - y) + g_o\tau_v \qquad (9a)$$

$$V_z = \frac{g\,(\rho_\ell - \rho_v)}{\mu}(\delta_y - y/2) + \frac{g_o\tau_v y}{\mu} \qquad (10a)$$

$$\Gamma = \frac{g(\rho_\ell - \rho_v)}{\nu}\,\frac{\delta^3}{3} + \frac{g_o\tau_v}{\nu}\,\frac{\delta^2}{2} \qquad (11a)$$

Assuming a linear temperature distribution in the film and a uniform (averaged at some distance btween Z=0 and Z=Z_L, the plate height) one obtains the following non-dimensional formulation:-

$$Z^* = (\delta^*)^4 \pm \frac{4}{3}\tau_v^*\,(\delta^*)^3 \qquad (12a)$$

$$\frac{4\Gamma}{\mu}\,\frac{1}{(1-\rho_v/\rho_\ell)} = \frac{4}{3}(\delta_L^*)^3 + 2\tau_v^*(\delta_L^*)^2 \qquad (13a)$$

$$h^* = \frac{4}{3}\,\frac{(\delta_L^*)^3}{Z_L^*} + \frac{2\tau_v^*(\delta_L^*)^2}{Z_L^*} \qquad (14a)$$

where:-

$$\delta^* = \delta\left(\frac{g}{\nu^2}\right)^{\frac{1}{3}} \qquad (15a)$$

$$Z^* = \frac{4Z\Delta T}{Pr} \frac{c_p}{h_{fg}'} \left(\frac{g}{\nu^2}\right)^{\frac{1}{3}} \frac{1}{(1 - \rho_v/\rho_\ell)} \tag{16a}$$

$$\tau_v^* = \frac{g_o \tau_v}{g(\rho_\ell - \rho_v)\ (\nu^2/g)^{\frac{1}{3}}} \tag{17a}$$

$$h^* = \frac{h}{k} \left(\frac{\nu^2}{g}\right)^{\frac{1}{3}} \tag{18a}$$

This results in a four-dimensional representation of h* versus Re with τ_v^* as a parameter and a new plot for each Prandtl Number (see Figure 8).

Modification to Present Case

A re-examination of the basic derivation indicates how the analysis might be modified for horizontal tubes with significant pressure gradients in the flow direction. In equation (9), the term $g(\rho_\ell - \rho_v)(\delta - y)$ represents the gravitational body force on the film ($\rho_\ell g$) with a correction for the hydrostatic pressure gradient in the vapor ($-\rho_v g$). In an internal flow situation, the vapor-phase pressure gradient should be replaced by the true pressure gradient.

$$F_o = \left(\frac{dP_v}{dz}\right)_{frict.} + \left(\frac{dP_v}{dz}\right)_{mom.} + \left(\frac{dP}{dz}\right)_{grav.}$$

Repeating the analysis with this corrected pressure gradient, equations (9a) through (18a) become the following (numbered as 9b through 18b for ease of comparison):

$$\frac{\mu dV_Z}{dy} = g_o F_o (\delta - y) + g_o \tau_v \tag{9b}$$

$$V_Z = \frac{g_o F_o}{\mu} (\delta y - \frac{y^2}{2}) + \frac{g_o \tau_v y}{\mu} \tag{10b}$$

$$\Gamma = \frac{g_o F_o}{\nu} \frac{\delta^3}{3} + \frac{g_o \tau_v}{\nu} \frac{\delta^2}{2} \tag{11b}$$

Equation (12b) is identical with Equation (12a) but the starred terms have new definitions.

$$\frac{4\Gamma}{\mu} = \frac{4}{3} (\delta_L^*)^3 + 2\tau_v^* (\delta_L^*)^2 \tag{13b}$$

$$h^* = \frac{4}{3} \frac{(\delta_L^*)}{Z_L^*} + \frac{2\tau_v^* (\delta_L^*)^2}{Z_L^*} \tag{14b}$$

where:-

$$\delta^* = \delta (\frac{g_o F_o}{\nu \mu})^{\frac{1}{3}} \tag{15b}$$

$$Z^* = \frac{4Z\Delta T}{Pr} \frac{c_p}{h_{fg}'} (\frac{g_o F_o}{\nu \mu})^{\frac{1}{3}} \tag{16b}$$

$$\tau_v^* = \frac{\tau_v}{F_o (\frac{\mu \nu}{g_o F_o})^{\frac{1}{3}}} \tag{17b}$$

$$h^* = \frac{h}{k} (\frac{\nu \mu}{g_o F_o})^{\frac{1}{3}} \tag{18b}$$

In retrospect by comparing the results of the two analyses the change from the old equations to the new may be accomplished by:-

$$\text{replacing } \frac{\nu^2}{g} \quad \text{by} \quad \frac{\nu\,\mu}{g_o F_o}$$

$$\text{and replacing } g(\rho-\rho_v) \text{ by } g_o F_o$$

Then the graphs from reference [29] reproduced here as Fig. 8 may be used with h* given by Equation (18b) and τ_v^* by Equation (17b). The abscissa remains $Re = 4\Gamma/\mu$.

The above corrected analysis applies to the laminar film. Inspection of the equations for transition and for the turbulent film analysis in reference [29] suggest the above transformations should apply there equally well. This analysis will be presented in detail in the future.

The pressure drop terms of F_o may be calculated as follows: The local friction pressure drop as recommended by Soliman et al [31] is:-

$$\frac{g_o D(dp/dZ)_f}{2G^2/\rho_v} = 0.045\left(\frac{GD}{\mu_v}\right)^{-0.2}\left[x^{1.8} + 5.7\left(\frac{\mu_\ell}{\mu_v}\right)^{0.0523}(1-x)^{0.47}x^{1.33}\left(\frac{\rho_v}{\rho_\ell}\right)^{0.261} + 8.11\left(\frac{\mu_\ell}{\mu_v}\right)^{0.105}(1-x)^{0.94}x^{0.860}\left(\frac{\rho_v}{\rho_\ell}\right)^{0.522}\right] \qquad (19)$$

This equation must be integrated along the tube knowing the quality vs. length to obtain the overall pressure drop.

The momentum term in F_o suggested by Soliman et al [31] is:-

$$\frac{g_o D(dp/dZ)_{mom}}{2G^2/\rho_v} = \frac{1}{2} D \frac{dx}{dZ} \left[2(1-x)\left(\frac{\rho_v}{\rho_\ell}\right)^{\frac{2}{3}}\right.$$

$$+ \left(\frac{1}{x} - 3 + 2x\right)\left(\frac{\rho_v}{\rho_\ell}\right)^{\frac{4}{3}} + \left(2x-1-\beta x\right)\left(\frac{\rho_v}{\rho_\ell}\right)^{\frac{1}{3}}$$

$$\left. + \left(2\beta - \frac{\beta}{x} - \beta x\right)\left(\frac{\rho_v}{\rho_\ell}\right)^{\frac{5}{3}} + 2(1-x-\beta+\beta x)\frac{\rho_v}{\rho_\ell}\right] \qquad (20)$$

where $\beta = 1.25$ for turbulent flow.

Here again the equation must be integrated along the length.

In these tests the gravity term is omitted because the tube was horizontal. Also for the test conditions, the momentum term is always less than 5% of the friction term.

DISCUSSION OF RESULTS

The data for the 24 test runs are tabulated in Appendix C and plotted in the 11 sub-graphs of Figure 4. The heat balance is a comparison of the enthalpy change of refrigerant through both the test section and the after-condenser with the cooling water enthalpy rise in both units. The heat balance is within 5% except for runs 4, 13, 20 and 21. The graph for each of the test runs appears at least once in Figure 4. Many of the runs appear on more than one of the graphs. The three major independent variables are the mass velocity, G, the pressure level or saturation temperature, T_{sat}, and the temperature difference between vapor and wall $T_v - T_{wall}$. Actually it is difficult to compare raw data as plotted in Figure 4 because the saturation temperature varies along the length of the tube because of pressure drop and the temperature difference varies along the length of the tube because the cooling water temperature was essentially the same at all stations. On each one of the graphs of Figure 4 the magnitude of the inlet saturation temperature, the cooling water temperature, the mass velocity and the range of temperature differences along the tube are listed. The five plots in the A-series generally show the strong influence of mass velocity. The six plots in the B-series attempt to show the effect of pressure level at the same flow rate. From the 24 runs made, it was not possible to show clearly the effect of the level of temperature difference.

In addition, the various runs were plotted over a Baker (36) flow regime map, Figure 5. It should be noted that the Baker flow

regime boundaries were drawn for isothermal flow; further, the boundaries are not very precise but should be drawn as fairly wide bands. It is not at all certain that these same boundaries are applicable to this non-isothermal flow with condensation at the wall. No flow regime maps have been made for this case. Inspection of Figure 5 shows that the high flow runs are likely to be in the dispersed-annular flow regime; the lower flow runs may be in annular flow with a dry core; and some runs may go into the slug-flow regime in the downstream sections.

Graphs A-2 and A-5 show clearly the effect of flow velocity. The increased flow velocity produces a higher heat transfer coefficient all along the tube. Fig. A-3 shows two runs at essentially the same conditions. The agreement appears to be within around 5%.

Fig. B-1 tends to show the effect of pressure level. The curves tend to be higher as T_{sat} increases. A similar result seems to be shown by Fig. B-6.

It is interesting to note on Fig. A-1 that the curves for very high flow rates cross the curves for the lower flow rates. From the flow regime map of Figure 5, these high flow rate curves may be in dispersed annular flow in the upstream section and dry-core annular flow in the downstream section. In dispersed annular flow there are liquid droplets in the core; hence, less liquid would be on the wall than there would be if the flow had been dry-core annular. This plus the effect of the high core velocity in thinning the liquid film produces higher heat transfer coefficients in the upstream portion.

The liquid droplets in the core travel much faster than the liquid on the wall, therefore, the actual quality is very much less than the flowing quality. This core liquid is carried downstream and deposited on the wall when the flow returns to dry-core annular, thus producing a much thicker liquid layer on the wall. This may explain why the high and low flow curves cross each other.

A number of the runs at the lower flow rates go to rather low qualities at the exit and may go through slug flow to 100% liquid flow. The heat transfer coefficient curves for these runs appear to level off at higher h values. This may be due to the fact that since the slugs of liquid fill the tube the liquid films in the vapor sections are much thinner than would be expected if the flow had remained annular.

Again it should be remembered that these discussions regarding flow regime are speculative since the regime boundaries may be quite different for condensing flows.

In analyzing the data runs 4, 13, 20 and 21 should be viewed with caution because the heat balances are off by more than 5%, possibly due to a flow measurement error.

All six test sections had a wall thermocouple installed at the side, 90 degrees from the top of the tube. The third section, in addition, had wall thermocouples at the top and bottom of the tube. The difference in these wall temperatures at any time was always less than $0.8^{\circ}F$.

Pressure taps were installed at both ends of each of the six sections of the test tube. The readings were not valid because the lines had

varying amounts of liquid and vapor fractions. In the future the manometers will be lowered to attempt to have the lines filled with liquid.

Between each of the six sections a 3-inch long transparent section was installed to attempt to observe flow regimes. The observations were difficult to interpret because of the cylindrical shape. It was estimated that annular flow existed most of the time. During some low flow rate runs there appeared to be large waves or perhaps slugs at the downstream end at low qualities. These observations could not be made with any degree of certainty, however.

ERROR ANALYSIS

The cooling water flow rate was determined by weigh-tanks. We estimate the error in that flow rate to be of the order of 0.25%. We estimate the error in the cooling water temperature rise to be of the order 2.75% or the error in the heat flux to be around 3%. The estimate of the error in the temperature difference between vapor and inside wall temperature is around 2%, therefore, the error in the heat transfer coefficient would be the sum of these two - or around 5%.

The inherent error in the freon vapor flow meter is stated by the manufacturer to be 2%. Fluctuations in the float reading were of the order of $\pm$ 1%. Therefore, the maximum error in the freon flow reading would be approximately 3%. This, along with the estimated 3% error in the heat flux, would produce an error in the change in quality from the inlet of about 6%.

COMPARISON WITH ANALYSIS

The data was compared with other data and the proposed correlation of Akers and Rosson [2] as recommended in the ASHRAE Guide, Figure 6. The data taken here lies above the Akers and Rosson suggested equations and is about at the same level as the data of Chen [14].

Figure 7 is a comparison of data on the correlation scheme recommended by Brauser [10]. On this plot the present data tends to lie in the vicinity of the Chen and Altman et al [3] but lies lower than the data of Brauser.

The data was further compared with predictions of average heat transfer coefficient from the graphs of Figure 8 with h* given by Equation (18b) and τ_v* by Equation (17b). The values of h* were read from each of the graphs - for Pr = 1 and Pr = 10, and the results obtained by interpolating linearly with Pr to the magnitude for R-12 which is in the range of 3.5 to 4.

The results are shown in Figure 9 as measured vs predicted values of h. The agreement is always within $\pm$ 15% and much closer for most runs. Runs 4, 13, 20 and 21 were omitted because of poor heat balance.

The local values of h are compared with the Boyko-Kruzhilin Equation (7) and are plotted in Figure 10 as measured vs. predicted values. It is seen that the agreement of the present local measurements and the prediction of Equation (7) is not very good. The measured results are usually higher than the Equation (7) predictions. In some cases the

predictions are low in the high quality region and high in the low quality region. See also Figure 11.

Some of the runs at lower flow rates go down to average qualities in the last section of around 3% to 5%. In these cases the measured h values (average for the last section of the apparatus) are 2 to 4 times the magnitude predicted for single phase all liquid flow, suggesting a rapid drop in h as the fully condensed region is approached.

CONCLUSIONS

1. Twenty test runs with heat balances error of less than 5% appear to provide good data and agreement with a proposed prediction method. Four runs (4, 13, 20 and 21) are suspect because of heat balance error (13 to 22%).

2. The data falls in the general range of other data on an Akers & Rosson plot, Figure 6, and on a Brauser plot, Figure 7. They are higher than the ASHRAE recommended Equations (4) and (5).

3. The earlier analysis for average heat transfer coefficient (Rohsenow, Webber and Ling [29]) was modified for horizontal flow to include total pressure drop effect. This modified analysis using the method of Soliman et al [31] to calculate the pressure drop terms gave agreement with the test data within $\pm$15%.

4. The Boyko-Kruzhilin prediction, Equation (7) does not agree well with the measured values of h (Figure 10), obtained in these experiments.

RECOMMENDATIONS:

1. Since the modification of the Rohsenow, Webber, Ling analysis was based on the details of the laminar flow region, the prediction method proposed here must be considered a tentative one. The entire analysis

must be re-done to include the total pressure drop both in the laminar and turbulent regions. Solutions will be accomplished on the computer.

2. Further the analysis should be performed step-wise along a tube starting with various inlet conditions and permitting F_o and τ_v to vary along the length as was done by Lehtinen [22]. This will provide predictions for the local coefficients. This produces multiparametered results. Effort must be devoted to simplifying these results after they are obtained.

3. The present test runs are for a 0.493" ID tube with R-12 condensing. Future work will involve testing at 0.8" and 0.2" ID of both R-12 and R-22.

4. The proposed prediction method is based on a dry-core annular flow regime model. Analysis for bubbly flow, slug flow and dispersed annular flow regimes will be studied.

REFERENCES

1. Akers, W.W., H.A. Deans and O.K. Crosser, "Condensing Heat Transfer Within Horizontal Tubes", Chem. Eng. Prog. pp. 54-89 (1958)

2. Akers, W.W. and H.F. Rosson, "Condensation Inside a Horizontal Tube", Chem. Eng. Prog. - Symposium Series, Heat Transfer - Storrs, No. 30, Vol. 56, 1960.

3. Altman, M., F.W. Staub and R.H. Norris, "Local Heat Transfer and Pressure Drop for Refrigerant-22 Condensing in Horizontal Tubes", ASME-AIChE, Storrs, Conn., August 1959.

4. Altman, M., F.W. Staub and R.H. Norris "Local Heat Transfer and Pressure Drop for Refrigerants Evaporating in Horizontal Tubes" Journal of Heat Transfer, A.S.M.E. August 1960.

5. Ananiev, E.P., L.D. Boyko and G.N. Kruzhilin, "Heat Transfer in the Presence of Steam Condensation in a Horizontal Tube", Int. Heat Transfer Conference Vol. II, pp. 290, 1961.

6. ASHRAE Handbook and Fundamental, 1967.

7. Bankoff, S.G. "A Variable Density Single-Fluid Model for Two-Phase Flow with Particular Reference to Steam-Water Flow" ASME Trans. Vol. 82, pp. 265, 1960.

8. Borchman, J., "Heat Transfer of High Velocity Vapors Condensing In Annuli", Trans. ASHRAE, No. 2023, Feb. 1967.

9. Boyko, L.D. and G.N. Kruzhilin, "Heat Transfer and Hydraulic Resistance during Condensation of Steam in a Horizontal Tube and in a Bundle of Tubes", Int. Journal of Heat Transfer and Mass Transfer. Vol. 10, pp. 361, March 1967.

10. Brauser, S.O. "Turbulent Condensation In a Horizontal Tube", PhD Thesis, Department of Mechanical Engineering, Kansas State University, 1966.

11. Carpenter, E.F. and A.P. Colburn, "The Effect of Vapor Velocity on Condensation Inside Tubes" Proceedings of the General Discussion of Heat Transfer, I. Mech.E and ASME, July 1951.

12. Chaddock, J.B. "Film Condensation of Vapor in Horizontal Tubes". Sc.D. Thesis, M.I.T. 1955.

13. Chato, S.C. "Laminar Condensation Inside Horizontal and Inclined Tubes" ASHRAE Journal, Feb. 1962.

14. Chen, Ching-Jen, "Condensing Heat Transfer in a Horizontal Tube", MS Thesis, Department of Mechanical Engineering, Kansas State University 1962.

15. Chen, M.M. "An Analytical Study of Laminar Film Condensation", Trans. ASME, Series C, Journal of Heat Transfer 83, No. 1, pp. 48, Feb. 1961.

16. Dickson, A.J. and S.W. Gouse, Jr., "Heat Transfer and Fluid Flow Inside a Horizontal Tube Evaporator. Final Report". Report No. DSR 9649, M.I.T. August 1966.

17. Dormer, T., Jr. and A.E. Bergles "Pressure Drop with Surface Boiling in Small-Diameter Tubes" Report No. 8767-31, Dept. of Mechanical Engineering, M.I.T. September 1964.

18. Dukler, A.E. "Fluid Mechanics and Heat Transfer in Vertical Falling-Film System", Chem. Eng. Pro. Sym. Series, Vol. 56, No. 30, 1960.

19. Goodykoontz, J.H. and R.G. Dorsch, "Local Heat Transfer Coefficients for Condensation of Steam in Vertical Downflow", NASA TN D-3326 March 1966.

20. Hilding, W.E. and C.H. Coogan, Jr. "Heat Transfer Studies of Vapor Condensing at High Velocity in Small Straight Tubes" NASA CR-124.

21. Hoogendoorn, C.J. "Gas-Liquid Flow in Horizontal Pipes" Chem. Eng. Science, Vol. 9, No. 1, Feb. 1959.

22. Lehtinen, J.A. "Film Condensation in a Vertical Tube Subject to Varying Vapor Velocity", Sc.D. Thesis, May 1957.

23. Lockhart, R.W. and R.C. Martinelli, "Proposed Correlation of Data for Isothermal Two-Phase, Two-Component Flow in Pipes", Chem. Eng. Progress, No. 1, pp. 39, 1959.

24. Martinelli, R.C. and D.B. Nelson "Prediction of Pressure Drop During Forced Circulation Boiling of Water" ASME Trans. Vol. 70, pp. 695-702, August 1948.

25. Moore, F.D. and R.B. Mesler, "The Measurement of Rapid Surface Temperature Fluctuation During Nucleate Boiling of Water" AIChE Journal, Vol. 7, pp. 620, 1961.

26. Patel, S.P. "Film Coefficient of Heat Transfer of Freon-12 Condensing Inside a Single Horizontal Tube" M.S. Thesis, Kansas State University 1956.

27. Rohsenow, W.M. "Heat Transfer and Temperature Distribution In Laminar-Film Condensation" Trans. ASME Vol. 78, No. 8, pp. 1645-1649, November 1956.

28. Rohsenow, W.M. and H.Y. Choi. "Heat, Mass and Momentum Transfer" Prentice-Hall Inc., 3rd printing 1965.

29. Rohsenow, W.M., J.H. Webber and A.T. Ling "Effect of Vapor Velocity on Laminar and Turbulent-Film Condensation", Trans. ASME, November 1956, (Paper No. 54-A-145).

30. Rosson, H.F. and J.A. Myers "Point Value of Condensing Film Coefficients Inside a Horizontal Pipe", 7th National Heat Transfer Conference, Aug. 1964.

31. Soliman, M., J.R. Schuster and P.J. Berenson "A General Heat Transfer Correlation for Annular Flow Condensation", ASME Paper No. 67-WA/HT-12, November 1967.

32. Tape, J.P. and A.C. Mueller "Condensation and Subcooling Inside an Inclined Tube", Chem. Eng. Progress, Trans., Vol. 43, pp. 267-278, May 1947.

33. Thermodynamic Properties of Freon-12" Du Pont

34. White, R.E. "Condensation of Refrigeration Vapors Apparatus and Film Coefficient for Freon-12", Trans. ASME, Vol. 70, 1948.

35. Zivi, S.M. " Estimation of Steady-State Steam Void-Fraction by Means of the Principle of Minimum Entropy Production" Journal of Heat Transfer, Trans. ASME, Series C., Vol. 86, No. 2, pp. 247-252, May 1964.

36. Baker, O. Oil and Gas Journal, November 10, 1958.

APPENDIX A

Tables of Data

RUN 1 G = 316,000 lb/hrft^2 $T_{water\ in}$ = 64.6

Sec No	Measured Values				Calculated Values				
	T_{vapor} °F	$T_{wall_{out}}$ °F	W_{water} lb/hr	$(T_{out}-T_{in})_w$ °F	$T_{wall_{in}}$ °F	(T_v-T_{sat}) °F	q/A $\frac{Btu}{hrft^2}$	h $\frac{Btu}{hrft^2 °F}$	x
1	94	78.8	1510	2.72	80.5	13.5	10,600	785	91.5
2	93.2	77.5	1450	2.49	79.0	14.2	9,350	658	75.2
3	92.4	76.6	1460	2.32	78.0	14.4	8,780	610	60.4
4	91.9	74.1	1930	1.69	75.5	16.4	8,440	514	46.4
5	90.2	72.7	1835	1.46	73.8	16.4	6,930	423	33.9
6	89.0	71.3	2170	1.17	72.4	16.6	6,560	396	22.1

Heat balance error = 2.9%

RUN 2 G = 354,000 lb/hrft^2 $T_{water\ in}$ = 64.4

Sec No	Measured Values				Calculated Values.				
	T_v	T_{wout}	W_w	ΔT_w	$T_{w,in}$	ΔT_v	q/A	h	x
1	96.0	81.9	2070	3.09	84.6	11.4	16,500	1,450	88.0
2	95.6	80.9	1120	3.42	82.5	13.1	9,900	755	68.6
3	95.1	78.4	1580	2.62	80.1	15.0	10,700	713	53.6
4	94.6	76.0	1600	2.22	77.5	17.1	9,200	538	39.1
5	94.0	73.6	1590	1.72	74.7	19.3	7,060	366	27.2
6	93.6	73.6	1375	1.80	74.6	19.0	6,400	337	17.3

Heat balance error = 0.8%

RUN 3 G = 468,000 $lb/hrft^2$ $T_{water\ in}$ = 64.4

Sec No	Measured Values				Calculated Values				
	T_{vapor} °F	$T_{wall_{out}}$ °F	W_{water} lb/hr	$(T_{out}-T_{in})_w$ °F	$T_{wall_{in}}$ °F	(T_v-T_{sat}) °F	q/A $\frac{Btu}{hrft^2}$	h $\frac{Btu}{hrft^2°F}$	x
1	97.0	84.4	2,070	3.47	87.4	9.6	18,600	1,940	81.6
2	95.8	84.0	1,120	4.06	85.9	9.9	11,800	1,190	73.0
3	95.0	7[illegible].7	1,580	2.89	81.6	13.4	11,800	880	59.9
4	93.9	77.0	1,600	2.42	78.6	15.3	9,960	652	46.3
5	93.0	75.9	1,590	2.17	77.4	15.6	8,910	572	37.5
6	91.0	75.4	1,475	2.02	76.4	14.3	7,700	548	27.8

Heat balance error = 2.7%

RUN 4 G = 360,000 $lb/hrft^2$ $T_{water\ in}$ = 67.9

Sec No	Measured Values				Calculated Values.				
	T_v	$T_{w_{out}}$	W_w	ΔT_w	$T_{w_{in}}$	ΔT_v	q/A	h	x
1	95.0	82.3	2,090	2.54	84.5	10.5	13,700	1,300	90.0
2	94.7	81.0	1,490	2,58	82.6	12.1	9,930	820	73.1
3	94.3	79.6	1,870	2.14	81.3	13.0	10,300	793	58.5
4	93.7	79.3	1,500	2.22	80.7	13.0	8,600	662	45.0
5	93.3	77.6	1,900	1.76	79.0	13.3	8,630	648	32.6
6	93.0	76.5	2,770	1.38	78.1	14.9	9,900	664	13.2

Heat balance error = 13.7%

RUN 5 G = 254,000 $lb/hrft^2$ $T_{water\ in}$ = 67.9

Sec No	Measured Values				Calculated Values				
	T_{vapor} °F	$T_{wall_{out}}$ °F	W_{water} lb/hr	$(T_{out}-T_{in})_w$ °F	$T_{wall_{in}}$ °F	(T_v-T_{sat}) °F	q/A $\frac{Btu}{hrft^2}$	h $\frac{Btu}{hrft^2 \cdot F}$	x
1	93.0	79.4	2,090	2.03	81.2	11.8	11,000	932	89.0
2	92.1	78.6	1,490	2.10	79.9	13.2	8,100	613	69.8
3	91.7	76.6	1,870	1.59	77.9	13.8	7,700	558	53.7
4	91.4	75.4	1,500	1.48	76.3	15.1	5,740	380	40.2
5	91.0	75.0	1,900	1.30	76.1	14.9	6,400	428	27.9
6	-	-	-	-	-	-	-	-	-

RUN 6 G = 265,000 $lb/hrft^2$ $T_{water\ in}$ = 67.9

Sec No	Measured Values				Calculated Values.				
	T_v	T_{wout}	W_w	ΔT_w	$T_{w_{in}}$	ΔT_v	q/A	h	x
1	99.0	81.8	2,090	2.44	84.0	15.0	13,200	879	87.0
2	97.8	80.1	1,490	2.38	81.6	16.2	9,150	565	65.2
3	97.3	77.8	1,870	1.80	79.2	18.1	8,700	478	47.4
4	96.9	76,8	1,500	1.74	77.9	19.0	6,750	355	32,2
5	96.5	75.5	1,900	1.39	77.6	19.9	6,830	344	19.0
6	96	74.0	2,770	1.00	75.2	20.8	7,160	344	3.5

Heat balance error = 1.5%

RUN 7 G = 155,000 $lb/hrft^2$ $T_{water\ in}$ = 51.4°F

Sec No	Measured Values				Calculated Values				
	T_{vapor} °F	$T_{wall_{out}}$ °F	W_{water} lb/hr	$(T_{out}-T_{in})_w$ °F	$T_{wall_{in}}$ °F	(T_v-T_{sat}) °F	q/A $\frac{Btu}{hrft^2}$	h $\frac{Btu}{hrft^2°F}$	x
1	84.6	67.2	1,760	2.32	68.9	15.7	10,600	675	82.8
2	84.2	62.7	1,500	1.92	63.7	20.3	7,450	367	53.8
3	83.8	62.4	1,610	1.78	63.6	20.2	7,400	366	29.7
4	83.5	60.5	1,900	1.40	61.6	21.9	6,870	314	8.8
5	82.0	58.2	2,260	0.84	59.2	22.8	5,840	256	-
6	79.4	55.2	2,360	0.56	55.8	23.6	3,440	143	-

Heat balance error = 4.9%

RUN 8 G = 445,000 $lb/hrft^2$ $T_{water\ in}$ = 51.6

Sec No	Measured Values				Calculated Values.				
	T_v	T_{wout}	W_w	ΔT_w	T_{win}	ΔT_v	q/A	h	x
1	87.8	72.6	2,670	2.82	74.9	12.9	20,150	1,560	88.6
2	86.7	68.9	2,470	2.30	71.3	15.4	14,700	955	68.7
3	85.7	66.7	2,300	2.18	68.8	16.9	13,000	768	53.0
4	85.1	66.2	1,730	2.31	67.9	17.2	10,350	602	39.8
5	84.5	63.4	2,050	1.78	65.0	19.5	9,430	484	28.8
6	84.0	60.4	2,260	1.28	61.6	22.4	7,500	335	19.3

Heat balance error = 1.9%

RUN 9 G = 440,000 lb/hrft^2 $T_{water\ in}$ = 51.4

Sec No	Measured Values				Calculated Values				
	T_{vapor} °F	$T_{wall_{out}}$ °F	W_{water} lb/hr	$(T_{out}-T_{in})_w$ °F	$T_{wall_{in}}$ °F	(T_v-T_{sat}) °F	q/A $\frac{Btu}{hrft^2}$	h $\frac{Btu}{hrft^2 °F}$	x
1	88.3	72.0	2,580	2.88	75.1	13.2	19,200	1,450	89.2
2	87.7	69.1	2,350	2.65	71.6	16.1	15,500	962	69.2
3	86.6	68.2	1,900	2.76	70.6	16.0	13,500	856	52.6
4	86.1	67.8	1,470	2.60	69.3	16.8	9,250	551	39.5
5	85.8	64.7	1,460	2.21	66.1	19.7	8,360	425	29.4
6	85.1	60.9	1,190	1.74	61.8	23.3	5,350	230	21.6

Heat balance error = 1.9%

RUN 10 G = 220,000 lb/hrft^2 $T_{water\ in}$ = 52.2

Sec No	Measured Values				Calculated Values.				
	T_v	$T_{w_{out}}$	W_w	ΔT_w	$T_{w_{in}}$	ΔT_v	q/A	h	x
1	102.0	73.6	1,970	3.01	76.1	25.9	15,300	590	81.6
2	101.7	69.2	2,230	2.50	71.6	30.1	14,400	478	42.8
3	101.0	66.7	2,230	2.12	68.7	32.3	12,200	378	14.5
4	98.8	61.6	1,860	1.47	62.3	36.5	7,060	194	-
5									
6									

RUN 11 G = 272,000 $lb/hrft^2$ $T_{water\ in}$ = 75.0

Sec No	Measured Values				Calculated Values				
	T_{vapor} °F	$T_{wall_{out}}$ °F	W_{water} lb/hr	$(T_{out}-T_{in})_w$ °F	$T_{wall_{in}}$ °F	(T_v-T_{sat}) °F	q/A $\frac{Btu}{hrft^2}$	h $\frac{Btu}{hrft^2°F}$	x
1	94.5	84.7	1,750	1.94	86.1	8.4	8,780	1,045	91.8
2	94.2	84.1	1,420	1.82	85.2	9.0	6,680	743	75.1
3	93.9	83.2	1,510	1.66	84.3	9.6	6,490	676	64.6
4	93.6	80.4	1,270	1.80	81.3	12.3	5,900	482	54.6
5	93.0	79.3	1,915	0.81	80.0	13.0	4,030	310	47.1
6	91.0	78.3	1,565	0.68	78.8	12.2	2,740	275	40.7

Heat balance error = 0.4%

RUN 12 G = 477,000 $lb/hrft^2$ $T_{water\ in}$ = 64.0

Sec No	Measured Values				Calculated Values.				
	T_v	T_{wout}	W_w	ΔT_w	T_{win}	ΔT_v	q/A	h	x
1	93.0	82.0	1,820	3.26	84.5	8.5	15,300	1,800	91.8
2	92.2	80.5	1,030	3.50	82.0	10.2	9,350	916	78.6
3	91.0	77.3	1,915	2.36	79.2	11.8	11,600	984	67.2
4	90.2	72.9	2,280	1.50	74.4	15.8	8,840	558	56.2
5	87.0	69.4	2,070	0.91	70.3	16.7	5,350	320	48.6
6	85.0	68.7	2,280	0.80	69.5	15.5	4,720	304	43.0

Heat balance error = 2.3%

RUN 13 G = 154,000 lb/hrft^2 $T_{water\ in}$ = 63.8

Sec No	Measured Values				Calculated Values				
	T_{vapor} °F	$T_{wall_{out}}$ °F	W_{water} lb/hr	$(T_{out}-T_{in})_w$ °F	$T_{wall_{in}}$ °F	(T_v-T_{sat}) °F	q/A $\frac{Btu}{hrft^2}$	h $\frac{Btu}{hrft^2 °F}$	x
1	97.0	76.9	2,800	2.04	79.3	17.7	14,700	831	75.3
2	96.2	73.5	2,030	1.62	75.0	21.2	8,850	417	35.6
3	95.7	72.6	1,590	1.67	73.7	22.0	6,840	311	9.6
4	95.2	71.1	1,850	1.30	72.1	23.1	6,220	269	-
5	95.0	70.0	2,390	1.03	71.1	23.9	6,360	266	-
6	90.0	68.0	1,730	0.78	68.6	21.4	3,480	163	-

Heat balance error = 17.2%

RUN 14 G = 326,000 lb/hrft^2 $T_{water\ in}$ = 63.9

Sec No	Measured Values				Calculated Values.				
	T_v	T_{wout}	W_w	ΔT_w	$T_{w_{in}}$	ΔT_v	q/A	h	x
1	98.5	81.8	1,870	3.20	84.3	14.2	15,500	1,090	87.7
2	98.1	80.7	1,310	3.33	82.6	15.5	11,300	728	66.4
3	97.9	78.9	1,660	2.80	81.0	16.9	12,000	710	47.8
4	97.5	76.1	1,950	2.16	77.9	19.4	10,800	556	29.5
5	97.0	73.3	1,760	1.53	73.5	23.5	6,990	298	15.8
6	96.5	80.6	2,280	1.12	81.7	24.8	6,600	266	4.4

Heat balance error = 2.7%

RUN 15 G = 425,000 $lb/hr ft^2$ $T_{water\ in}$ = 64.9

Sec No	Measured Values				Calculated Values				
	T_{vapor} °F	$T_{wall_{out}}$ °F	W_{water} lb/hr	$(T_{out}-T_{in})_w$ °F	$T_{wall_{in}}$ °F	(T_v-T_{sat}) °F	q/A $\frac{Btu}{hr ft^2}$	h $\frac{Btu}{hr ft^2 °F}$	x
1	99.0	83.9	2,240	3.20	86.9	12.1	18,600	1,540	88.7
2	98.5	81.4	2,720	2.45	84.2	14.3	17,200	1,200	66.8
3	97.8	80.0	2,120	2,60	82.3	15.5	14,200	916	47.5
4	97.4	77.8	2,870	2.00	80.2	17.2	14,800	860	29.8
5	96.5	74.7	2,140	1.67	76.2	20.3	9,210	454	15.1
6	96.4	72.8	2,380	1.30	74.1	22.3	8,000	359	4.5

Heat balance error = 3.9%

RUN 16 G = 372,000 $lb/hr ft^2$ $T_{water\ in}$ = 63.5

Sec No	Measured Values				Calculated Values.				
	T_v	T_{wout}	W_w	ΔT_w	$T_{w_{in}}$	ΔT_v	q/A	h	x
1	96.0	79.2	2,240	2.65	81.7	14.3	15,350	1,070	89.1
2	95.4	76.5	2,720	2.07	78.9	16.5	14,550	882	68.5
3	94.9	76.6	2,120	2.25	78.6	16.3	12,300	755	50.0
4	94.4	74.3	2,870	1.67	76.3	18.1	12,400	685	32.7
5	93.4	70.8	2,140	1.25	81.9	21.5	6,900	322	19.3
6	92.5	69.7	2,380	1.02	70.7	21.8	6,270	288	14.9

Heat balance error = 1.06%

RUN 17 G = 358,000 $lb/hrft^2$ $T_{water\ in}$ = 65

Sec No	Measured Values				Calculated Values				
	T_{vapor} °F	$T_{wall_{out}}$ °F	W_{water} lb/hr	$(T_{out}-T_{in})_w$ °F	$T_{wall_{in}}$ °F	(T_v-T_{sat}) °F	q/A $\frac{Btu}{hrft^2}$	h $\frac{Btu}{hrft^2°F}$	x
1	101.0	83.3	2,240	3.10	86.2	14.8	17,900	1,210	87.7
2	100.8	81.6	2,720	2.62	84.6	16.2	18,400	1,140	61.3
3	100.1	79.2	2,120	2.43	81.3	18.7	13,300	713	38.0
4	99.5	75.8	2,870	1.68	77.8	21.7	12,500	576	19.2
5	98.8	72.5	2,140	1.31	73.7	25.1	7,250	289	4.8
6	98.4	71.2	2,380	1.02	72.2	26.2	6,270	240	-

Heat balance error = 4%

RUN 18 G = 506,000 $lb/hrft^2$ $T_{water\ in}$ = 63.9

Sec No	Measured Values				Calculated Values.				
	T_v	$T_{w_{out}}$	W_w	ΔT_w	$T_{w_{in}}$	ΔT_v	q/A	h	x
1	91.0	79.4	2,200	2.64	81.8	9.2	15,000	1,630	92.4
2	90.3	76.7	1,970	2.24	78.5	11.8	11,400	965	79.3
3	89.0	74.7	2,210	1.90	76.4	12.6	10,800	856	67.7
4	88.1	75.0	1,880	1.98	76.6	11.5	9,650	839	57.7
5	87.0	73.0	1,490	1.74	74.1	12.9	6,700	519	49.4
6	86.0	71.4	1,340	1.50	72.2	13.8	5,200	377	43.5

Heat balance error = 0.9%

RUN 19 G = 556,00 $lb/hrft^2$ $T_{water\ in}$ = 62.9

Sec No	Measured Values				Calculated Values				
	T_{vapor} °F	$T_{wall_{out}}$ °F	W_{water} lb/hr	$(T_{out}-T_{in})_w$ °F	$T_{wall_{in}}$ °F	(T_v-T_{sat}) °F	q/A $\frac{Btu}{hrft^2}$	h $\frac{Btu}{hrft^2 °F}$	x
1	88.0	77.0	2,200	2.39	79.2	8.8	13,600	1,550	94.0
2	86.9	76.3	1,970	2.34	78.2	8.7	11,900	1,370	82.1
3	85.2	74.9	2,210	2.03	76.8	8.4	11,600	1,390	71.6
4	83.9	71.3	1,880	1.51	72.5	11.4	7,350	645	62.6
5	81.6	68.0	1,490	1.04	68.6	13.0	4,010	319	57.5
6	81.2	68.1	1,340	1.00	68.7	12.7	3,460	272	54.2

Heat balance error = 3.4%

RUN 20 G = 257,000 $lb/hrft^2$ $T_{water\ in}$ = 68.8

Sec No	Measured Values				Calculated Values.				
	T_v	T_{wout}	W_w	ΔT_w	$T_{w_{in}}$	ΔT_v	q/A	h	x
1	94.6	82.0	2,020	2.38	84.0	10.6	12,400	1,170	84.6
2	94.2	82.3	1,790	2.50	84.2	10.0	11,600	1,160	79.0
3	93.8	79.1	1,720	1.93	80.5	13.3	8,600	647	58.5
4	93.4	79.2	1,620	2.02	80.6	12.8	8,480	660	47.7
5	93.0	76.3	1,540	1.44	77.2	15.8	5,720	362	38.9
6	92.6	77.5	1,330	1.78	78.5	14.1	6,130	435	4.2

Heat balance error = 20.8%

RUN 21 G = 308,000 $lb/hr ft^2$ $T_{water\ in}$ = 68.8

Sec No	Measured Values				Calculated Values				
	T_{vapor} °F	$T_{wall_{out}}$ °F	W_{water} lb/hr	$(T_{out}-T_{in})_w$ °F	$T_{wall_{in}}$ °F	(T_v-T_{sat}) °F	q/A $\frac{Btu}{hr ft^2}$	h $\frac{Btu}{hr ft^2 \cdot F}$	x
1	104.2	88.7	2,020	3.38	91.7	12.5	18,500	1,480	84.0
2	103.9	90.4	1,790	3.26	92.8	11.1	15,100	1,360	55.4
3	103.6	83.8	1,720	2.81	85.8	17.8	12,500	703	25.7
4	103.2	83.8	1,620	2.47	85.5	19.7	10,700	543	14.6
5	102.8	78.0	1,540	1.78	79.1	23.7	7,090	299	3.0
6	102.4	78.9	1,330	2.05	80.0	22.4	7,050	315	-

Heat balance error = 22.8%

RUN 22 G = 307,000 $lb/hr ft^2$ $T_{water\ in}$ = 79

Sec No	Measured Values				Calculated Values.				
	T_v	$T_{w_{out}}$	W_w	ΔT_w	$T_{w_{in}}$	ΔT_v	q/A	h	x
1	109.0	91.8	1,870	2.33	93.6	15.2	11,250	740	90.2
2	108.1	91.8	1,710	2.39	93.5	14.6	10,600	723	71.2
3	107.9	90.9	1,450	2.32	92.3	15.6	8,700	553	54.3
4	107.7	90.6	1,420	2.26	91.9	15.8	8,300	525	39.4
5	107.5	89.6	1,400	2.09	90.8	16.7	7,560	453	25.5
6	107.2	89.2	1,270	2.07	90.3	16.9	6,800	402	13.0

Heat balance error = 4.9%

RUN 23 G = 314,000 $lb/hrft^2$ $T_{water\ in}$ = 79.5

Sec No	Measured Values				Calculated Values				
	T_{vapor} °F	$T_{wall_{out}}$ °F	W_{water} lb/hr	$(T_{out}-T_{in})_w$ °F	$T_{wall_{in}}$ °F	(T_v-T_{sat}) °F	q/A $\frac{Btu}{hrft^2}$	h $\frac{Btu}{hrft^2 \cdot F}$	x
1	110.5	95.8	1,870	2.77	97.0	13.5	13,400	992	88.6
2	110.0	94.5	1,710	2.79	96.5	13.5	12,300	914	66.5
3	109.6	93.7	1,450	2.78	95.4	14.2	10,400	734	44.5
4	109.2	92.6	1,420	2.56	94.1	15.1	9,400	623	31.2
5	108.8	91.4	1,400	2.36	92.8	16.0	8,550	534	14.7
6	108.4	91.0	1,270	2.36	92.3	16.1	7,750	482	3.7

Heat balance error = 4.3%

RUN 24 G = 327,000 $lb/hrft^2$ $T_{water\ in}$ = 79.1

Sec No	Measured Values				Calculated Values.				
	T_v	T_{wout}	W_w	ΔT_w	T_{win}	ΔT_v	q/A	h	x
1	118.7	97.5	1,870	3.32	100.1	18.6	16,100	865	86.5
2	118.4	98.2	1,710	3.57	100.8	17.6	15,800	896	59.4
3	118.1	96.4	1,450	3.38	98.4	19.7	12,700	643	35.6
4	117.8	92.9	1,420	2.69	94.5	23.3	9,870	424	16.6
5	117.5	88.9	1,400	2.12	90.1	27.4	7,670	280	4.1
6	117.1	88.9	1,270	2.00	90.0	27.1	6,560	242	-

Heat balance error = 4.7%

APPENDIX B

Data Reduction

The data obtained in the experiments are tabulated in Appendix A. The section numbers are given to every 3 ft. long section starting from the inlet. The local vapor saturation temperature, local inner-wall temperature and local heat flux must be known in order to calculate the local heat transfer coefficient:-

$$h = \frac{q/A}{\Delta T} \tag{B1}$$

The local vapor temperatures were measured by thermocouples at the centerline of the test section. Since the vapor temperatures do not change much (1 - 5°F), fluid properties are taken at the saturation temperature of the test section inlet.

Initial attempts to measure the inner-wall temperature directly were not successful. In order to prevent the presence of the thermocouple from affecting the measurement, very small thermocouples wire (36 gauge wire) was used. However, some of the thermocouples were broken during the soldering operation. The local inner-wall temperatures were calculated from the equation:-

$$\frac{q}{A} = \frac{2k_{\ell}(T_i - T_o)}{D \ln(D_o/D)} \tag{B2}$$

or:

$$T_i = T_o + \frac{qD \ln (D_o/D)}{A \quad 2k_t} \tag{B3}$$

where the thermal conductivity of the condenser tube wall, k_t, was assumed constant over the temperature changes encountered in the test. The outer-wall temperatures, T_o, were measured.

The local heat flux was computed from the temperature rise and the flow rate of the cooling water.

$$\frac{q}{A} = \frac{W_w c_{pw} \Delta T_w}{\pi DL} \tag{B4}$$

It was assumed that there is no heat loss from the cooling water to surroundings, and the measured temperature rise of the cooling water is the bulk temperature change.

Qualities for each short section were evaluated from a heat-balance. An arithmetic mean value of inlet and outlet qualities of each short section was taken as a local quality at the measuring point.

Sample Calculation:

Run 1 (Sec. 1) :

$$\frac{q}{A} = \frac{W_w . \Delta T_w . C_{pw}}{\pi D L} \qquad \text{(B4)}$$

D = .493 in.

L = 3 ft.

$$\frac{q}{A} = \frac{1510 \times 2.72}{3.14(\frac{0.493}{12}) \times 3}$$

$$= 10,600 \quad \text{Btu/hrft}^2$$

$$T_i = T_o + \frac{qD\ell n\ (\frac{D_o}{D})}{2kt} \qquad \text{(B5)}$$

$$T_i = 78.8 + \frac{10,600(\frac{0.493}{12})\ \ell n(\frac{0.675}{0.493})}{2 \times 40}$$

$$= 80.5 \quad °F$$

$$h = \frac{q/A}{\Delta T} = \frac{10,600}{94-80.5} = 785 \frac{\text{Btu}}{\text{hrft}^2 °F}$$

Quality:-

at inlet 100%

at outlet $x_{out} = 1 - \frac{q\ /h_{fg}}{G \frac{\pi}{4} D^2}$

$$= 1 - \frac{10,600 \times \pi(\frac{0.493}{12}) \times 3}{316,000 \times \frac{\pi}{4} (\frac{0.493}{12})^2 \times 56,858} = 0.83$$

$$x_m = \frac{100 + 83}{2} = 91.5$$

Sample Calculation For heat balance on Test Section and After-Condenser Combined:-

Run 1

Test Fluid side:-

$$W = 316{,}000 \frac{\pi}{4} \left(\frac{0.493}{12}\right)^2 = 419 \text{ lb/hr}$$

T_v at test section inlet = 94°F

at 94°F $h_{fg} = 56.858$; $h_{liq} = 29.663$

at 70.6°F $h_{liq} = 24.189$

$\Delta h = 56.858 + 29.663 - 24.189 = 62.332$

$Q = (419)(62.332) = 26{,}100$ Btu/hr

Cooling Water Side:

From Appendix A:-

1510 x 2.72	=	4110
1450 x 2.49	=	3610
1460 x 2.32	=	3390
1930 x 1.69	=	3260
1835 x 1.46	=	2680
2170 x 1.17	=	2540
Test Sect. q	=	19590 Btu/hr.

In the after condenser:-

Cooling Water ΔT = 2.16°F

Flow Rate W = 3380 lb/hr

$q = (2.16)(3380) =$ 7300 Btu/hr

Total q to cooling water = 19590 + 7300 = 26890 $\frac{Btu}{hr}$

Heat balance error = $\frac{26890 - 26100}{26890}$ = 2.9%

APPENDIX C

Sample Calculation of the Modified Analysis

Run 6:

$$Tsat_{IN} = 99°F$$

$$Gt = 26500 \text{ lbm/hrft}^2 \qquad \frac{\mu_\ell}{\mu_v} = \frac{0.59}{0.031} = 18.7$$

$$R_e = \frac{266{,}000}{0.031}\left(\frac{0.493}{12}\right) = 3.51 \times 10^5$$

$$\frac{\rho_v}{\rho_\ell} = \frac{3.2017}{78.923} = 0.0406$$

$$\frac{2G^2}{g_o D \rho_v} = \frac{2(266{,}000)^2}{4.17 \times 10^8 \left(\frac{0.493}{12}\right)(3.2017)} = 2.58 \times 10^3$$

Then Equation (19) becomes:-

$$\left(\frac{dp}{dz}\right)_{fr} = 8.95[x^{1.8} + 2.73(1-x)^{0.47}x^{1.33} + 2.08(1-x)^{0.94}x^{0.86}]$$

Equation (26) becomes:-

$$\left(\frac{dp}{dz}\right)_{mom} = (2.58 \times 10^3)\left(\frac{1}{2}\right)\left(\frac{0.493}{12}\frac{\Delta x}{\Delta z}\right)[0.236(1-x) + 0.014\left(\frac{1}{x} - 3 + 2x\right) + 0.344(2x - 1 - \beta x) + 0.0048\left(2\beta - \frac{\beta}{x} - \beta x\right) + 0.0812(1 - x - \beta + \beta x)$$

where $\beta = 1.25$

$\Delta x/\Delta z$ is obtained from the Tables of Data plotted. The magnitudes

are read from the graph at the mid-point of each section.

Sect. No.	x	$\Delta x/\Delta z$	$(\frac{dp}{dz})_{fr}$	$-(\frac{dp}{dz})_{mom}$	F_o
1	87.0	8.20	17.2	0.407	16.8
2	65.2	6.55	17.3	0.373	16.9
3	47.4	5.45	14.4	0.325	14.1
4	32.2	4.65	10.6	0.284	10.3
5	19.0	4.7	6.5	0.275	6.2
6	3.5	5.6	1.6	0.202	1.4
					65.7

$$F_o = [(\frac{dp}{dz})_{fr} + (\frac{dp}{dz})_{mom}]_{avg}$$

$$= \frac{65.7}{6} = 10.95 \text{ lbf/ft}^3$$

For thin liquid film $\tau_v = \frac{D}{4}(\frac{dp}{dz})_{fr} = \frac{0.493}{12x4} \times 10.969 = 0.116$

$$(\frac{\mu\nu}{g_o F_o})^{\frac{1}{3}} = (\frac{(0.59)^2}{78.923 \times 4.17 \times 10^8 \times 10.959})^{\frac{1}{3}} = 0.989 \times 10^{-4}$$

$$\tau_v^* = \frac{0.116}{10,969} \times \frac{1}{0.989 \times 10^{-4}} = 107$$

$$Re = \frac{4\Gamma}{\mu} = 28,100$$

$h^* = 0.7$ for Pr = 1

$h^* = 2.0$ for Pr = 10

$h^* = 1.2$ for Pr = 3.5

$$\text{Then } h_{m_{pred}} = h^* \; k \left(\frac{g_o F_o}{\mu \nu}\right)^{\frac{1}{3}} = \frac{(1.2)(0.038)}{0.989 \times 10^{-4}} = 461$$

From the measurements on average h may be calculated two ways:-

$$h_{avg} = \frac{1}{6} \sum_{1}^{6} h_N = 494$$

$$h_{avg} = \frac{\frac{1}{6} \sum_{1}^{6} (q/A)_N}{\frac{1}{6} \sum_{1}^{6} (T_v - T_s)_N} = \frac{8632}{18.17} = 475$$

The latter one was used for comparison with the predicted value.

Comparison of Average h with Modified Analysis

Run No.	$havg_{meas}$*	$havg_{pred}$
1	553	545
2	630	650
3	883	815
5	564	515
6	474	454
7	378	320
8	721	690
9	677	690
10	475	410
11	535	540
12	700	767
14	550	535
15	800	819
16	624	636
17	556	547
18	815	782
19	824	806
22	562	514
23	675	575
24	513	478

$$*(havg)_{meas.} = \frac{\frac{1}{6}\sum_{n=1}^{6}(q/A)_n}{\frac{1}{6}\sum_{n=1}^{6}(\Delta T)_n}$$

LIST OF FIGURES

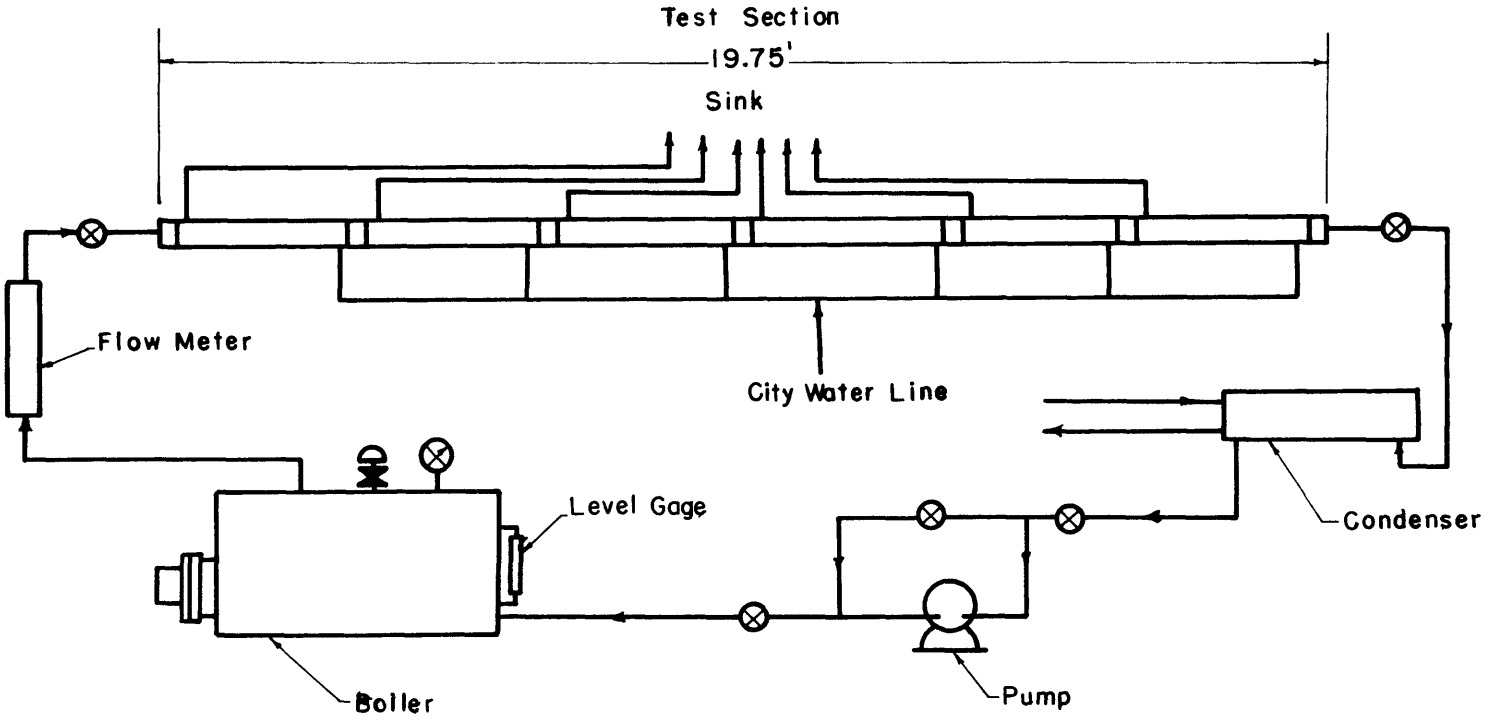

Fig. 1 Schematic Diagram of Apparatus

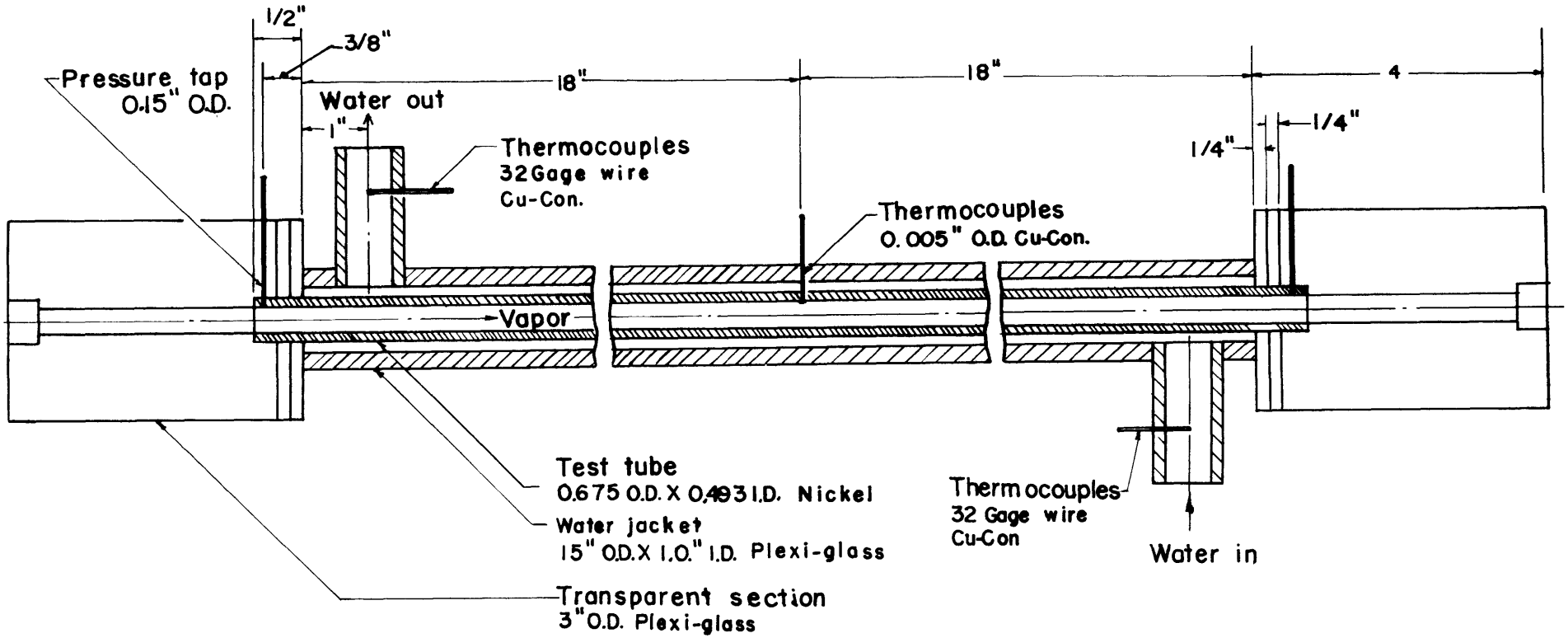

Fig. 2a. Schematic Drawing of one Section of the Test Section.

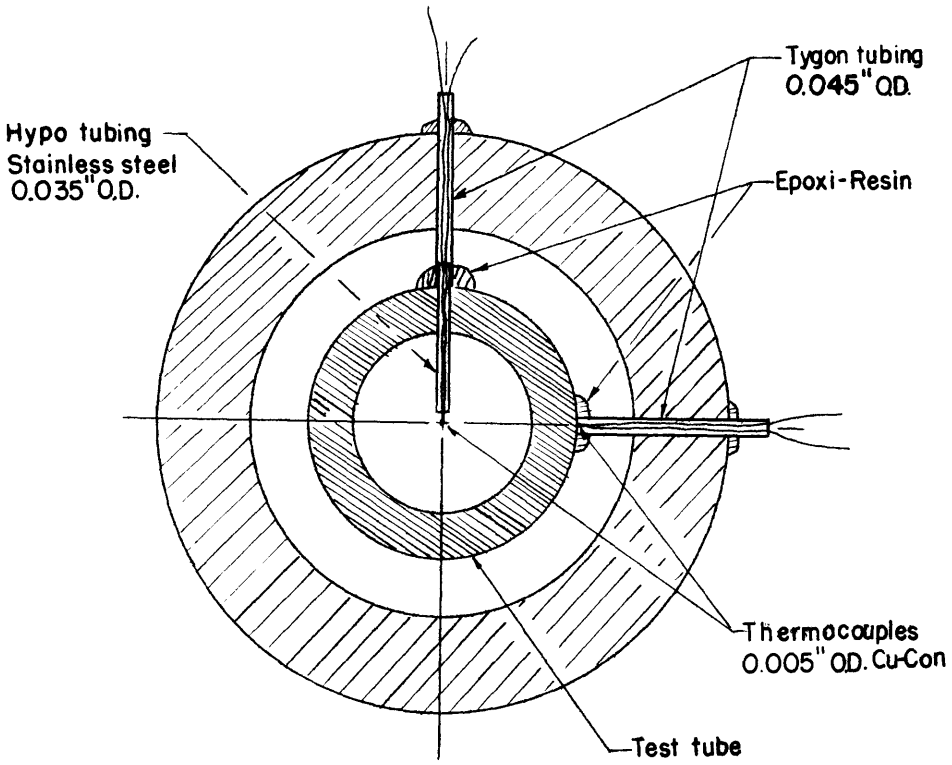

Fig. 2b. Thermocouple positioning

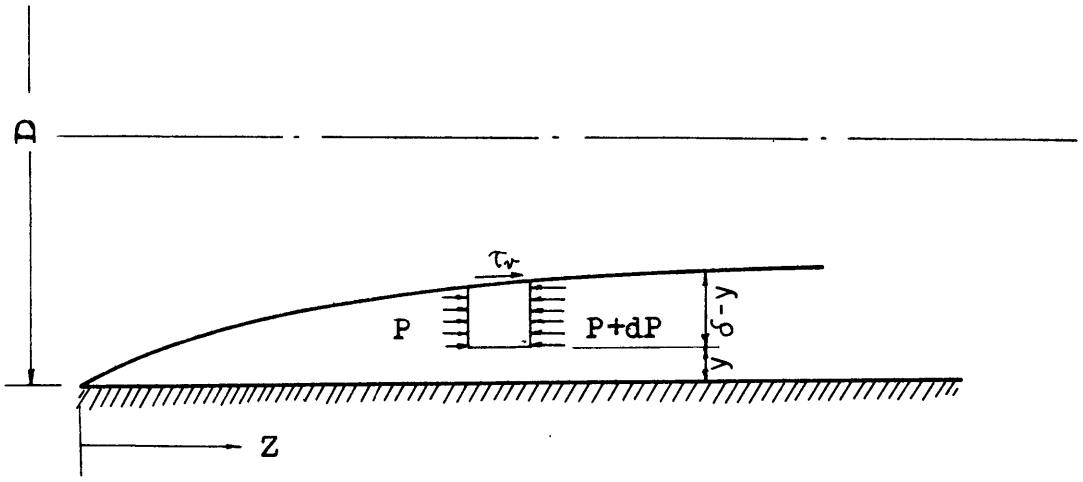

Fig. 3. Elemental Volume in Condensate Film

	$T_{SAT_{IN}}$	T_{WATER}	G	$T_v - T_{WALL}$
◐ Run 5.	93	67.9	254,000	11.8-15.1
◪ Run 20.	94.6	68.8	275,000	10.0-15.8
◒ Run 11.	94.5	75	272.000	8.4-13
◑ Run 4.	95	67.9	360,000	10.5-14.9
◓ Run 12.	93	64	477,000	8.5-16.7

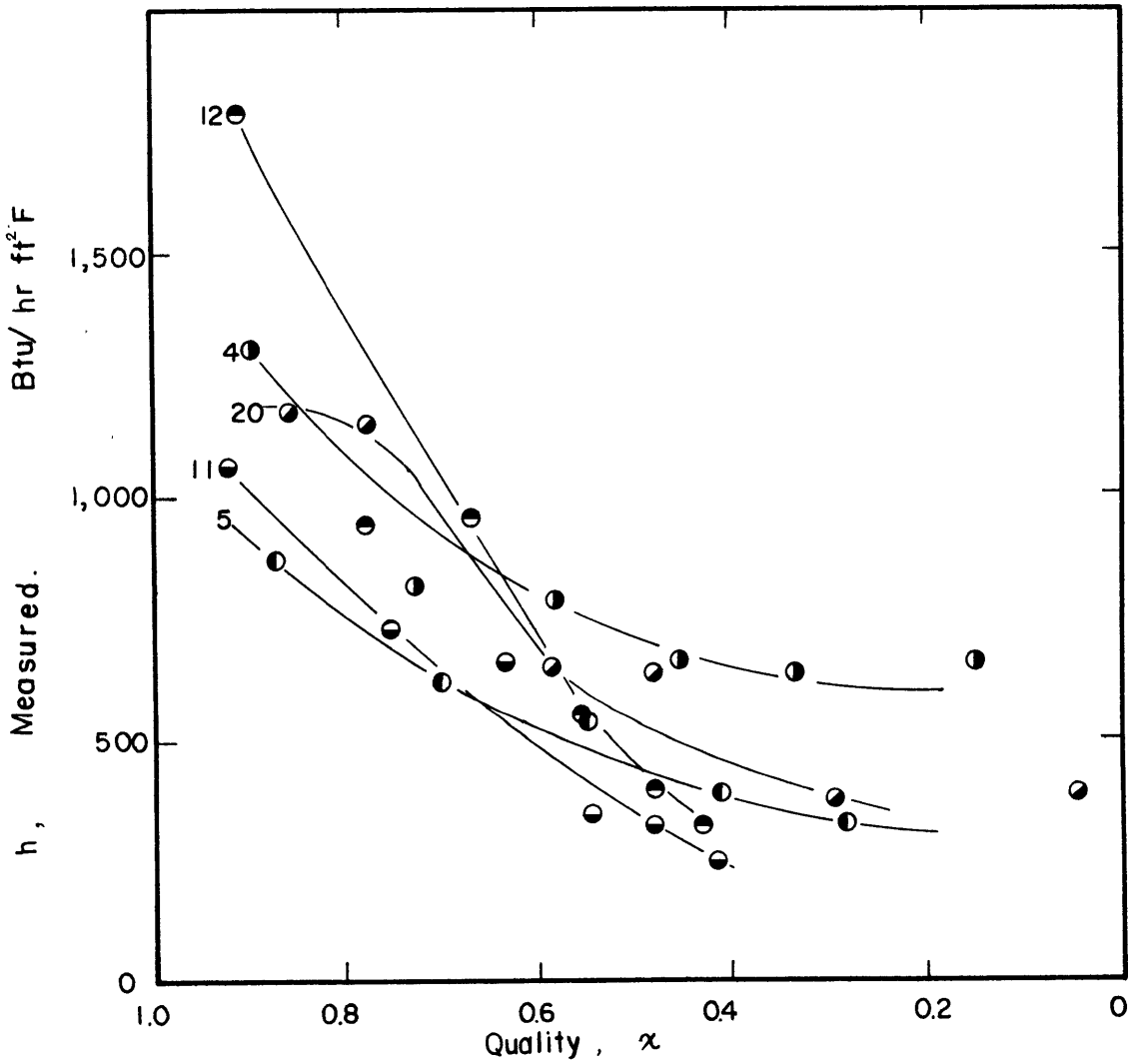

A - 1

Fig. 4. Measured h versus Quality

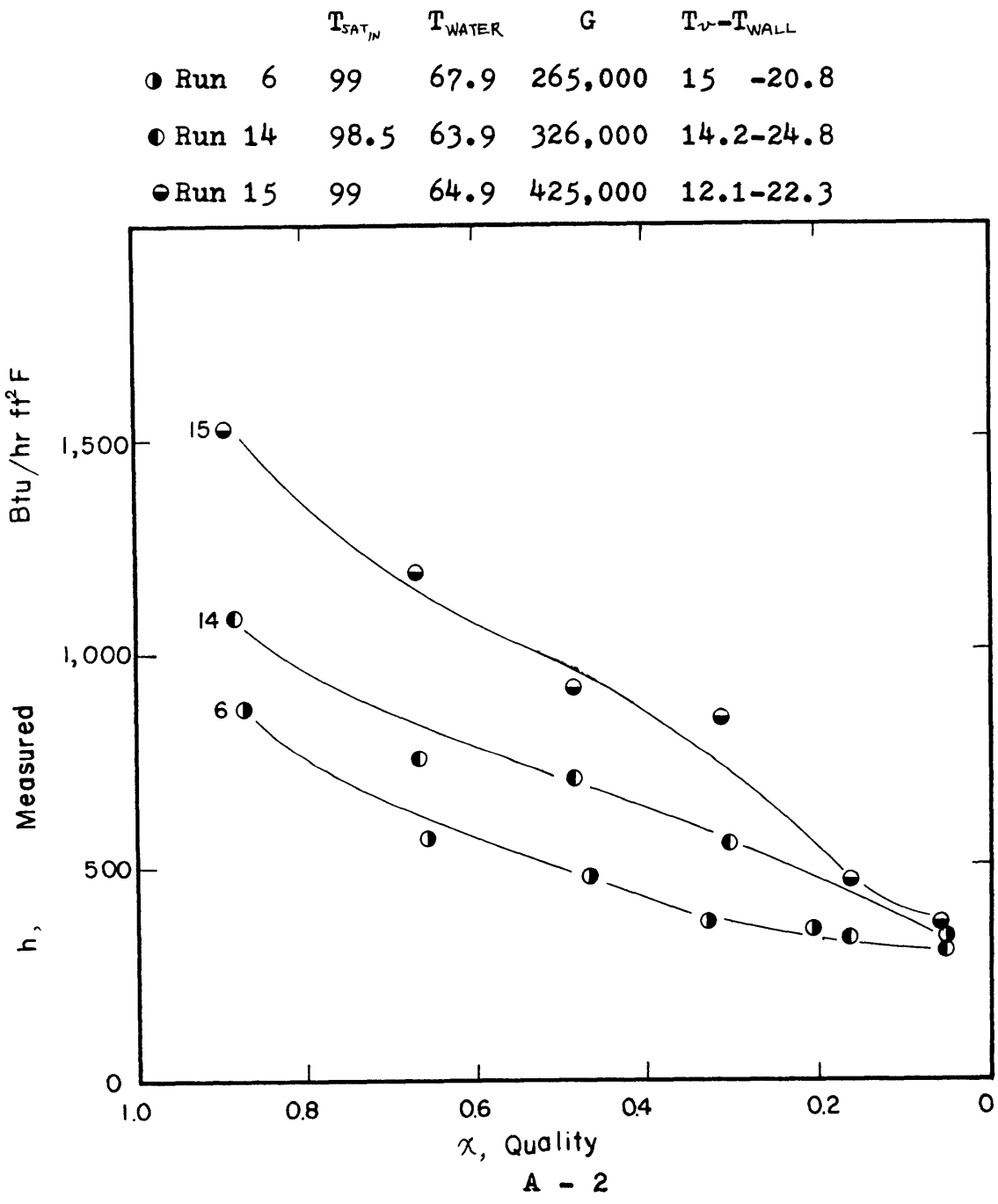

Fig. 4. Measured h versus Quality

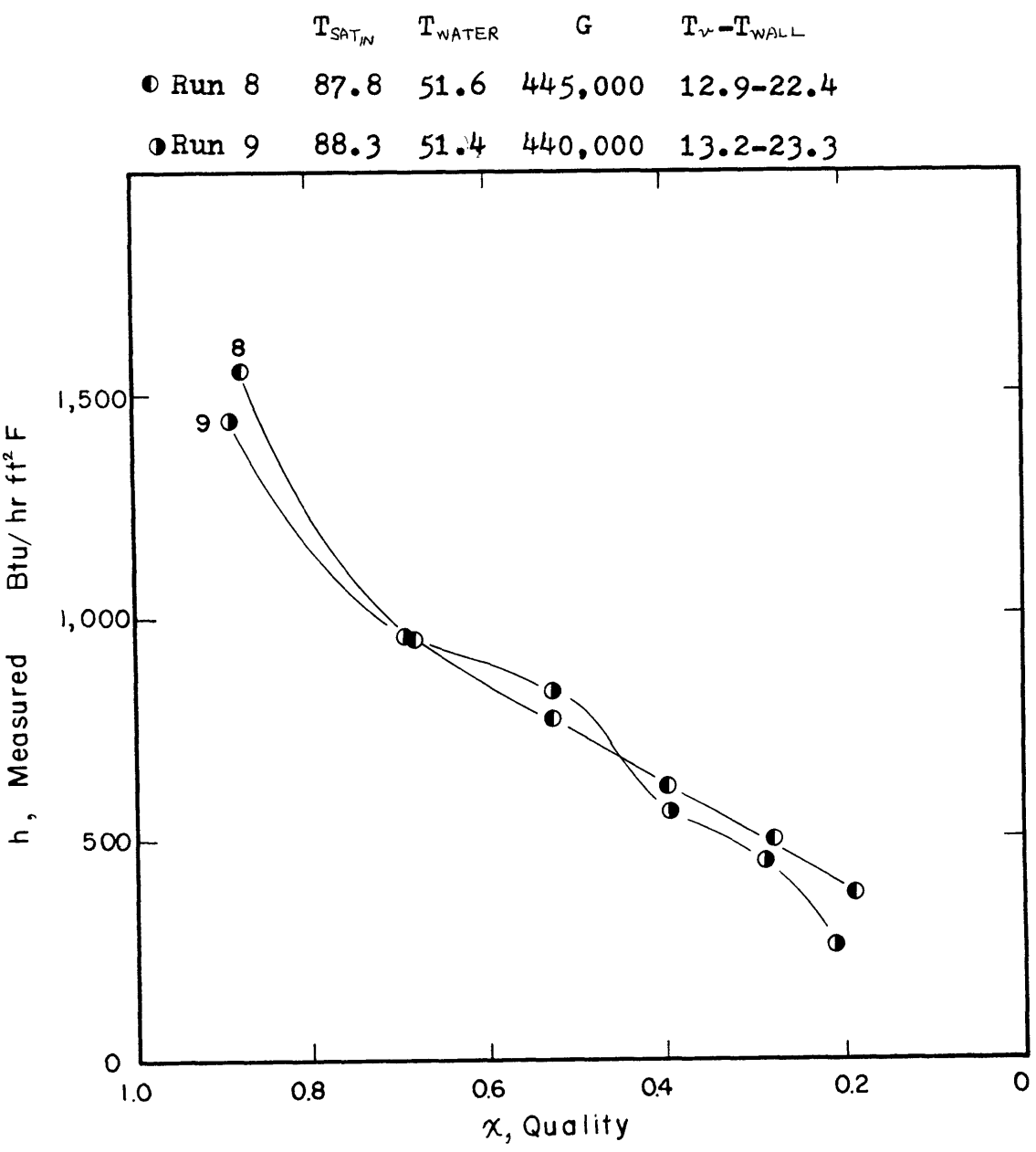

A - 3

Fig. 4. Measured h versus Quality

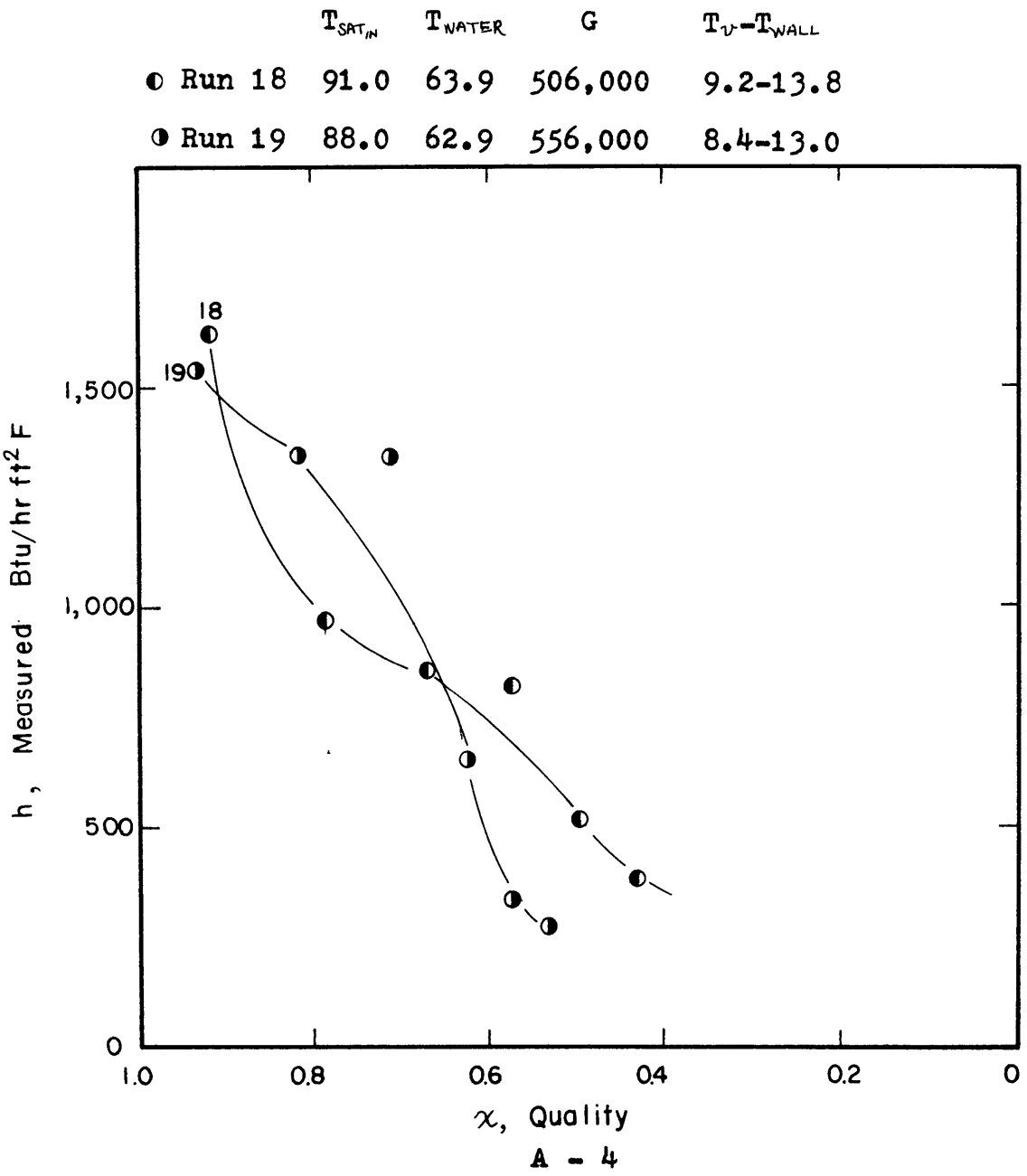

Fig. 4. Measured h versus Quality

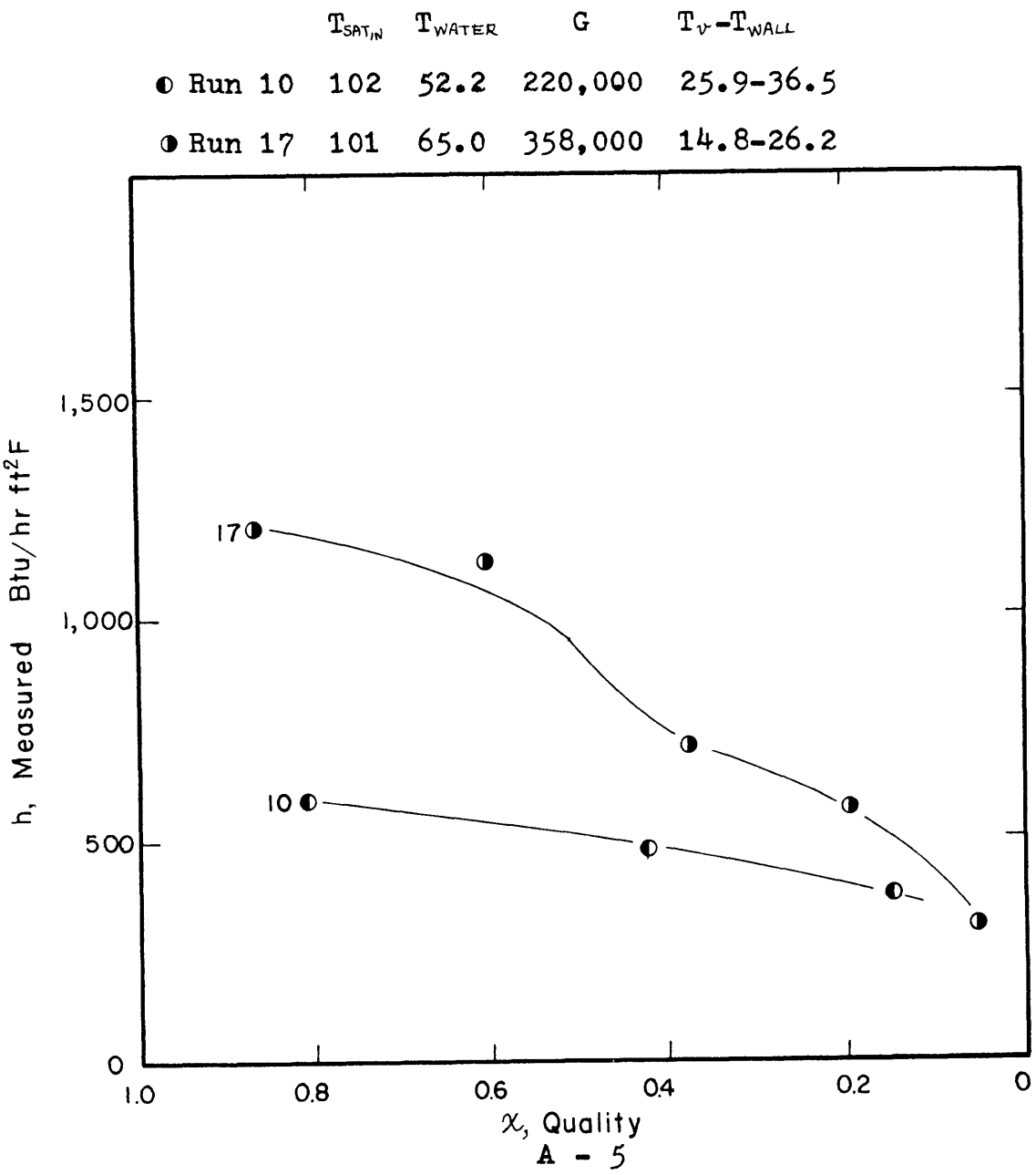

Fig. 4. Measured h versus Quality

	$T_{SAT_{IN}}$	T_{WATER}	G	$T_v - T_{WALL}$
◐ Run 14	98.5	63.9	326,000	14.2-24.8
◒ Run 16	96	63.5	372,000	14.3-21.8
◑ Run 23	110	79.5	314,000	13.5-16.1
● Run 24	118	79.1	327,000	17.6-27.4

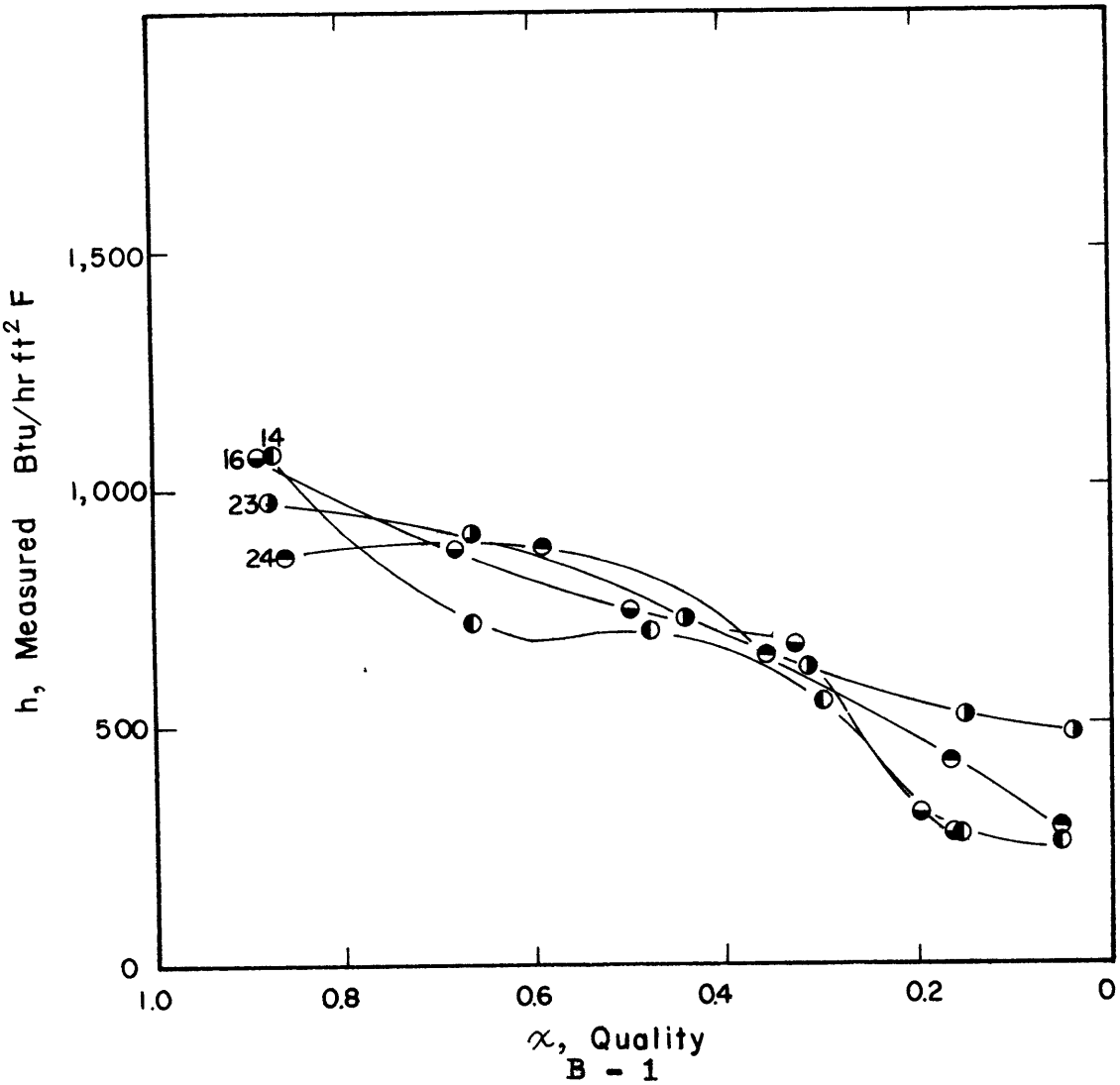

Fig. 4. Measured h versus Quality

	$T_{SAT_{IN}}$	T_{WATER}	G	$T_w - T_{WALL}$
◑ Run 1	94	64.8	316,000	13.5-16.6
◐ Run 21	88.7	68.8	308,000	11.1-23.7
◒ Run 22	109	79	307,000	14.6-16.9
◓ Run 23	110.5	79.5	314,000	13.5-16.1

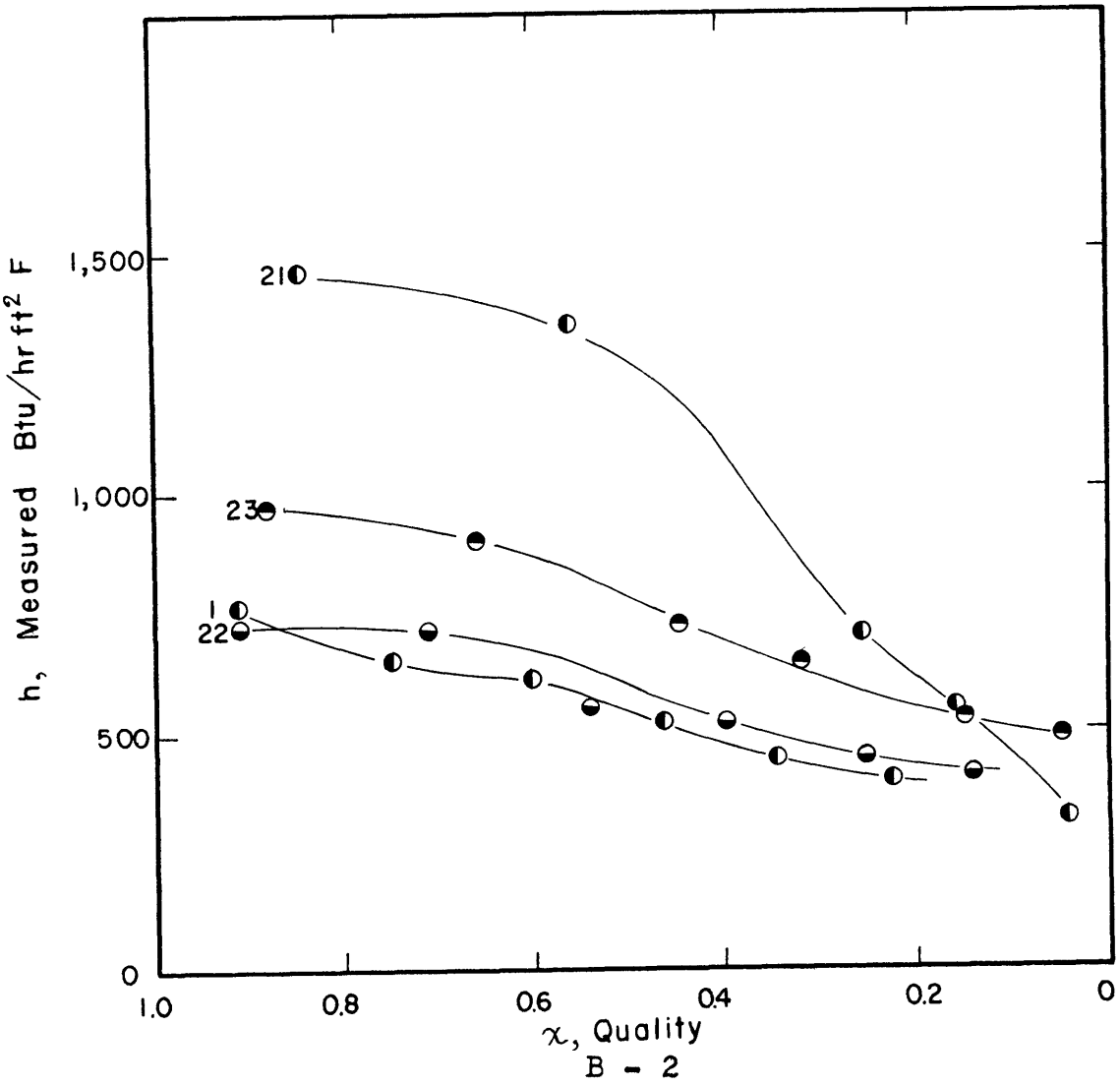

Fig. 4. Measured h versus Quality

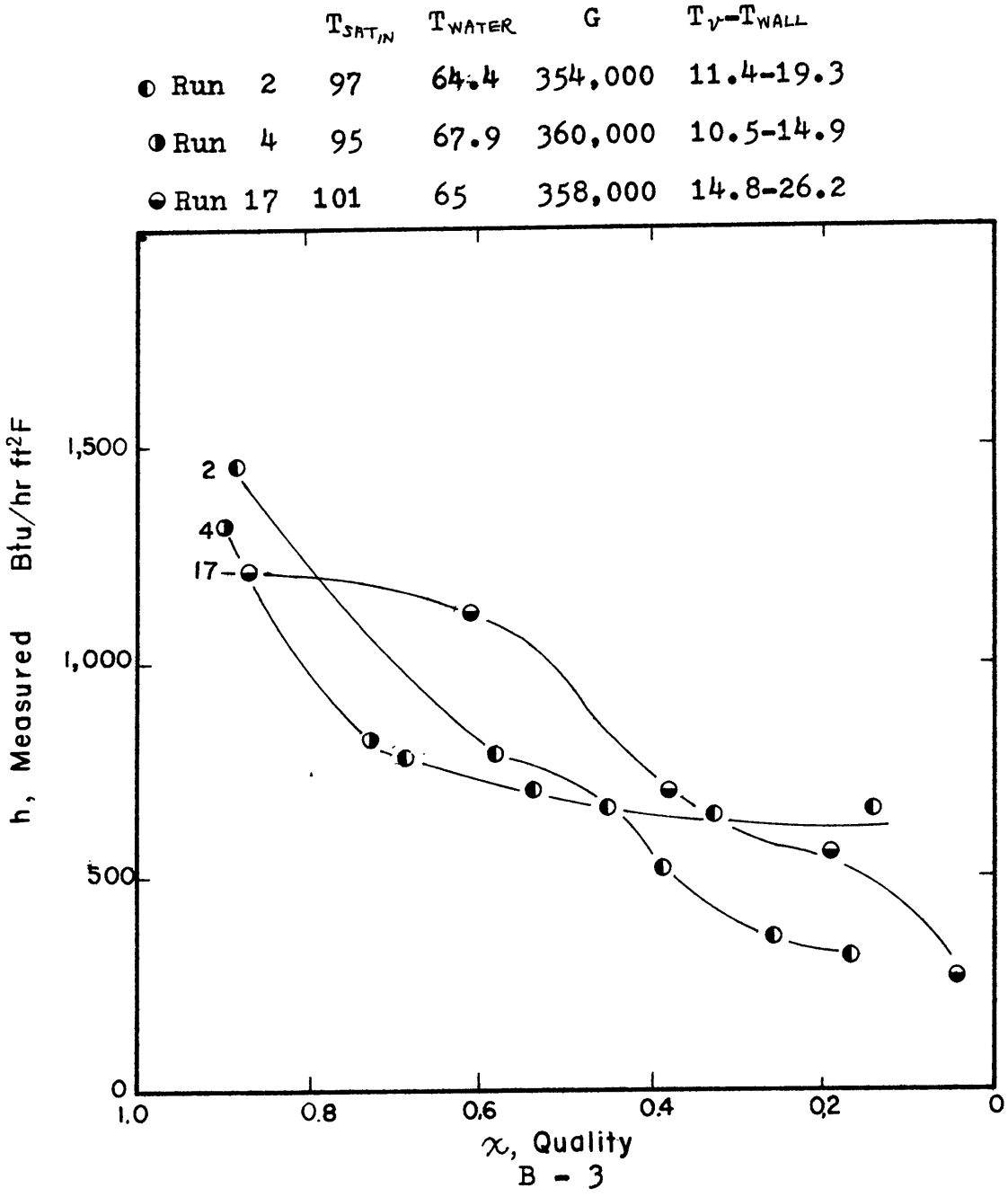

Fig. 4. Measured h versus Quality

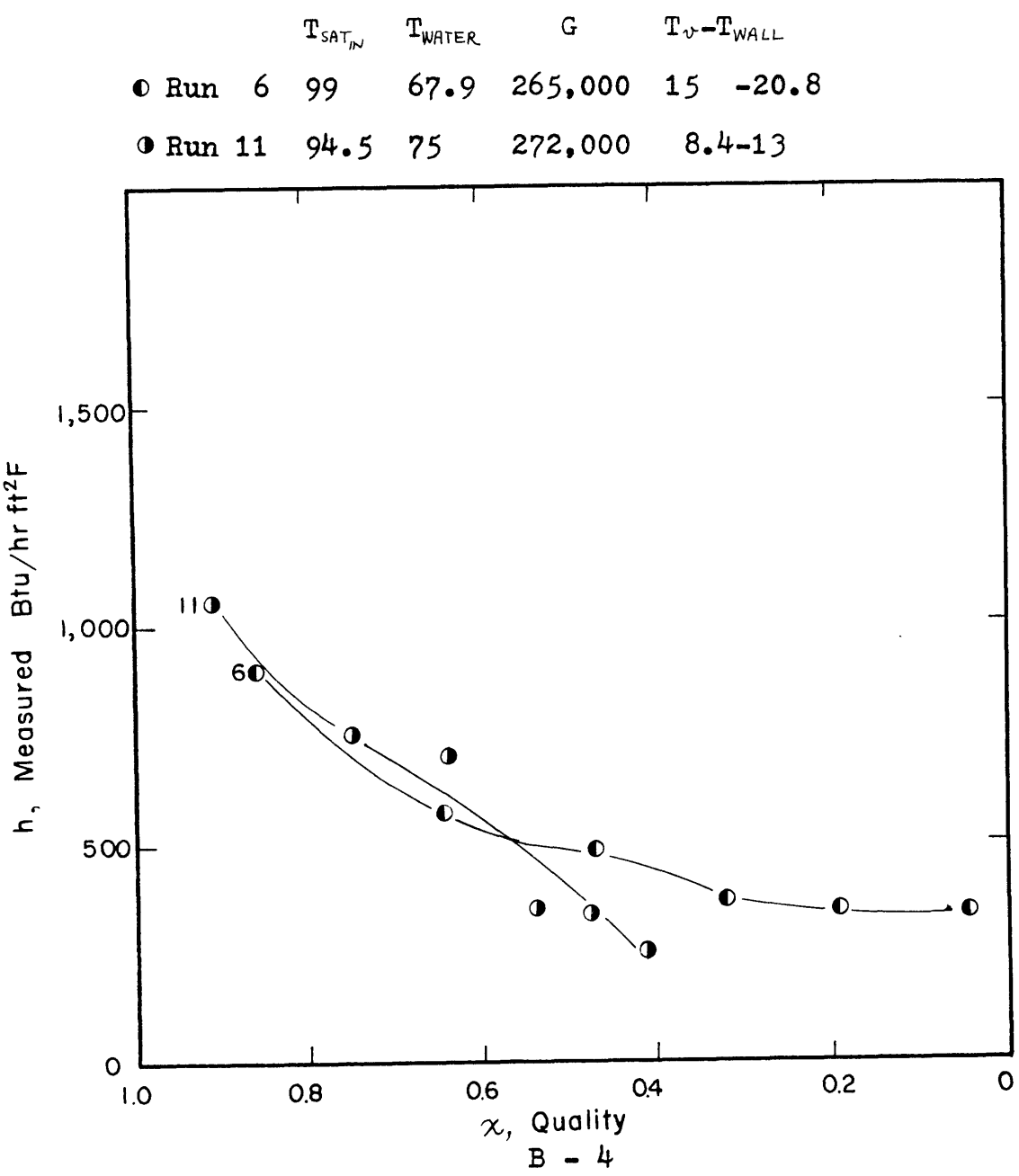

Fig. 4. Measured h versus Quality

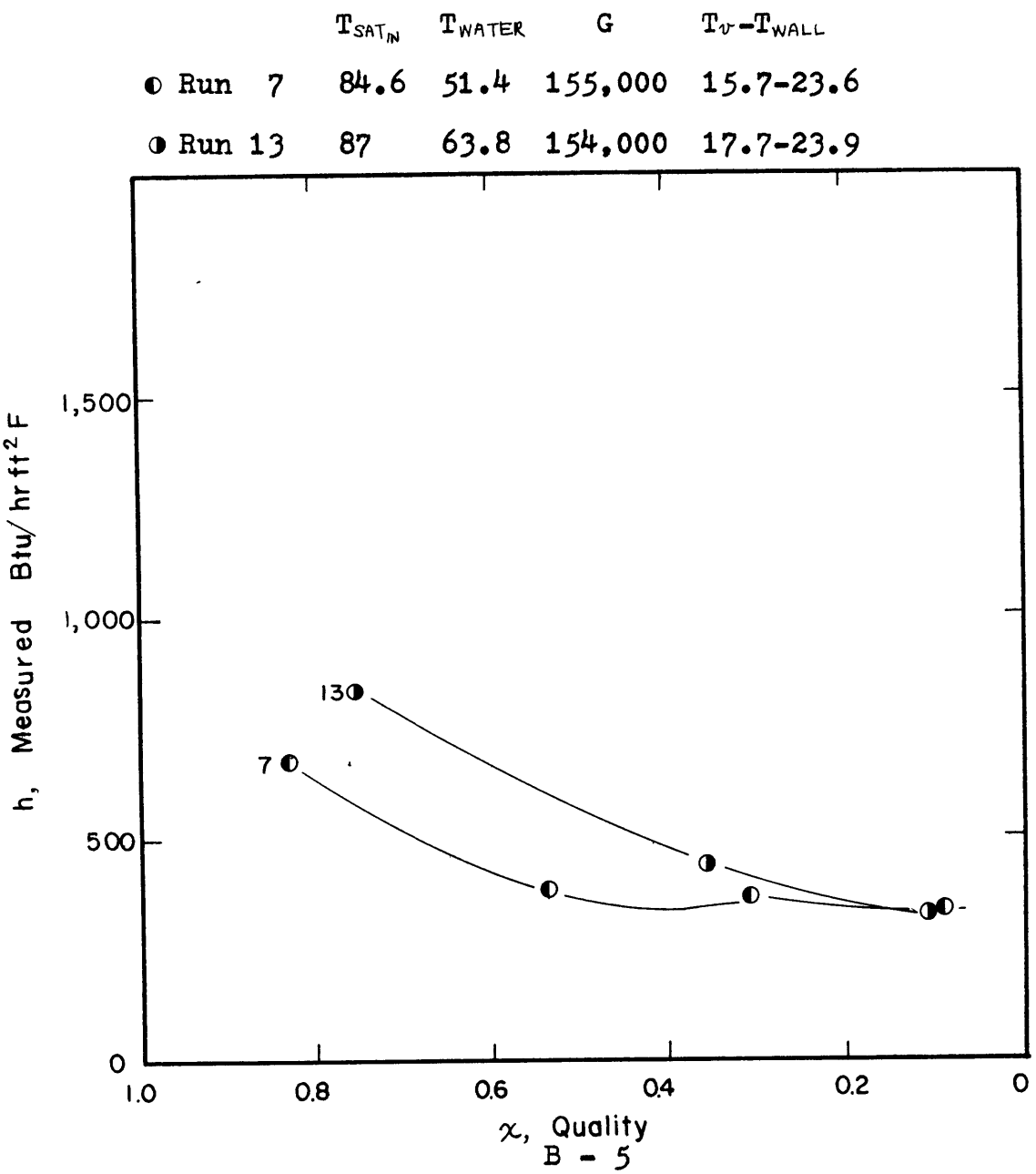

Fig. 4. Measured h versus Quality

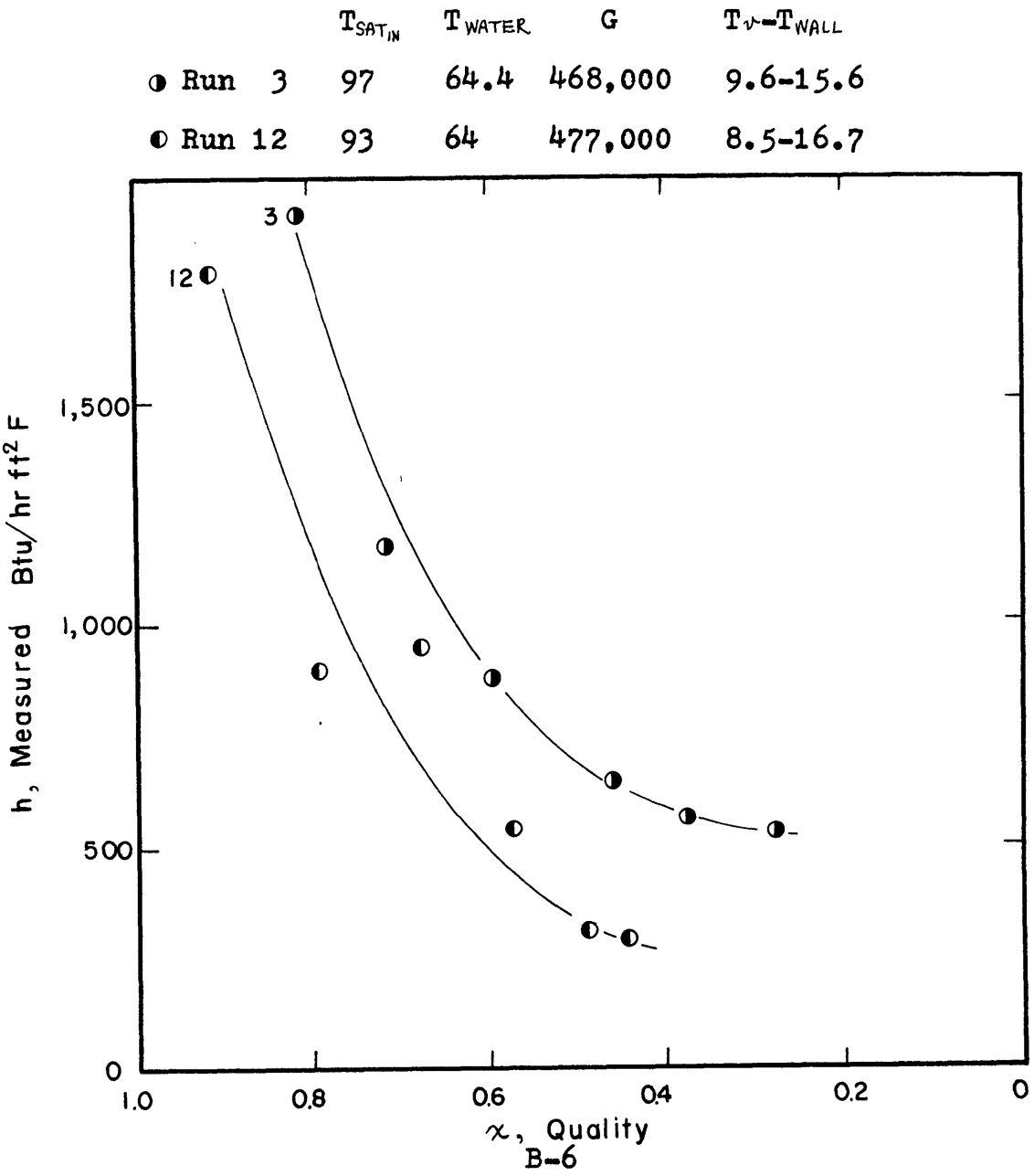

Fig. 4. Measured h versus Quality

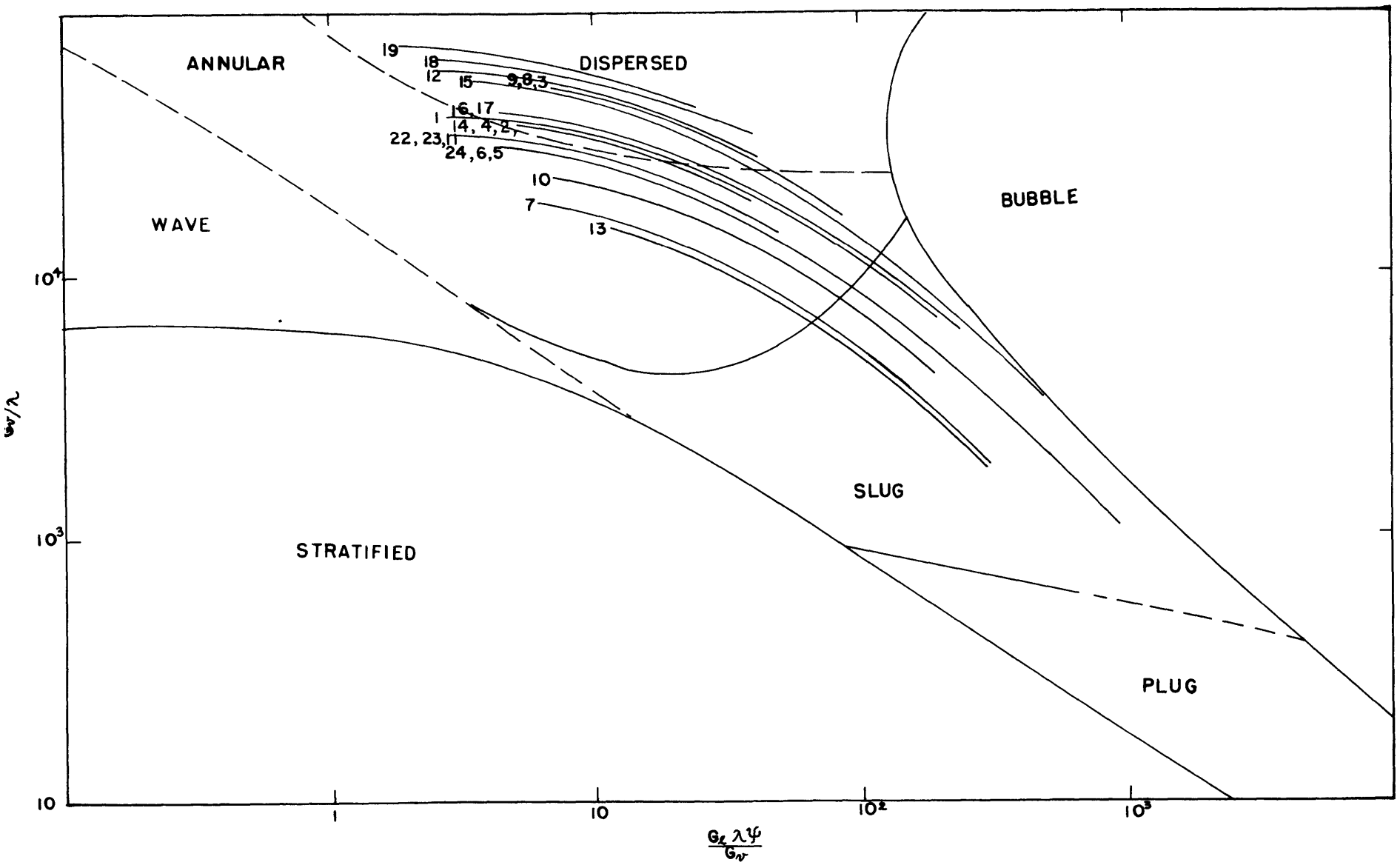

Figure 5. BAKER Flow Regime Map.

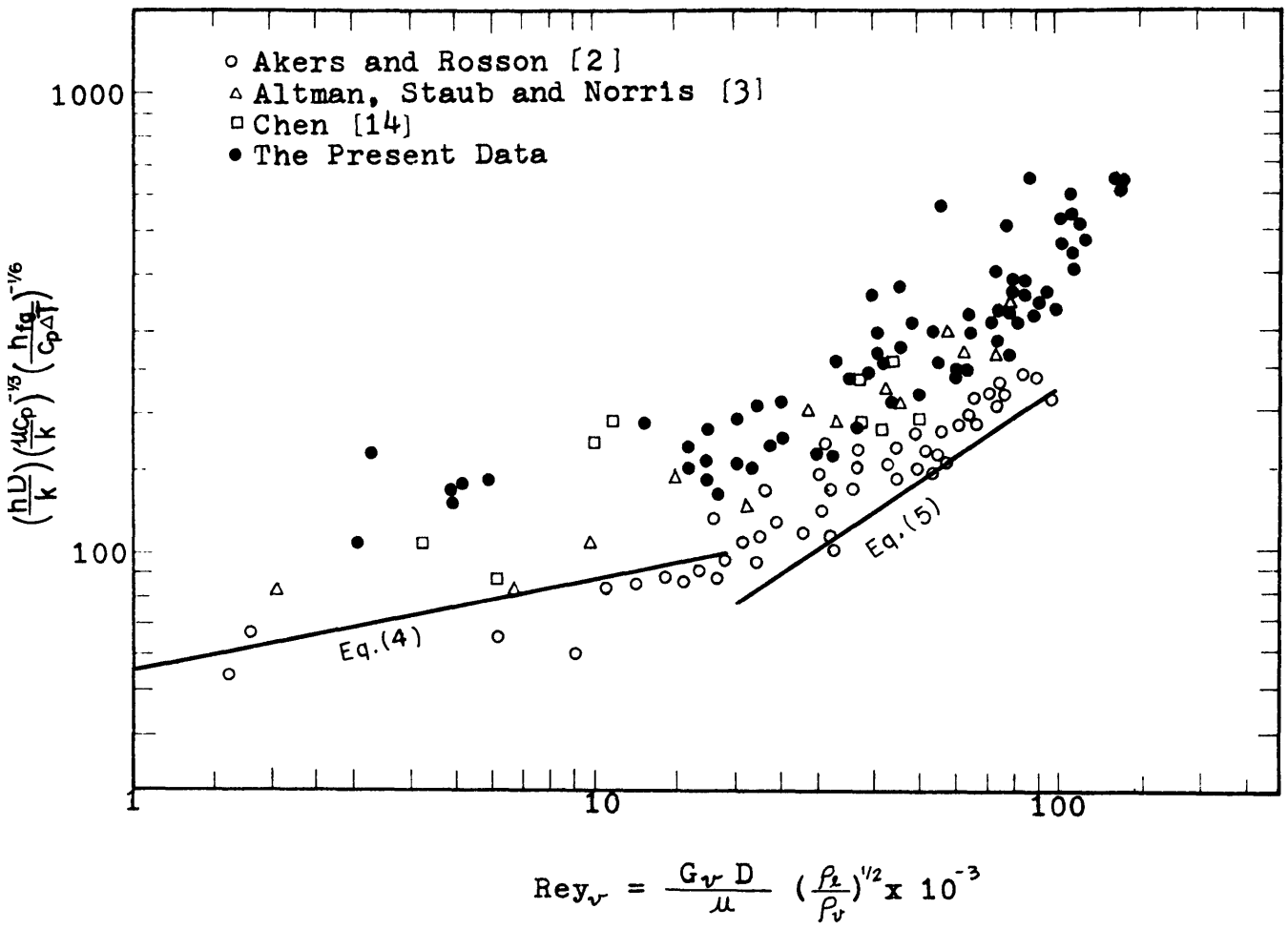

Fig. 6. Data on Akers-Rosson Plot

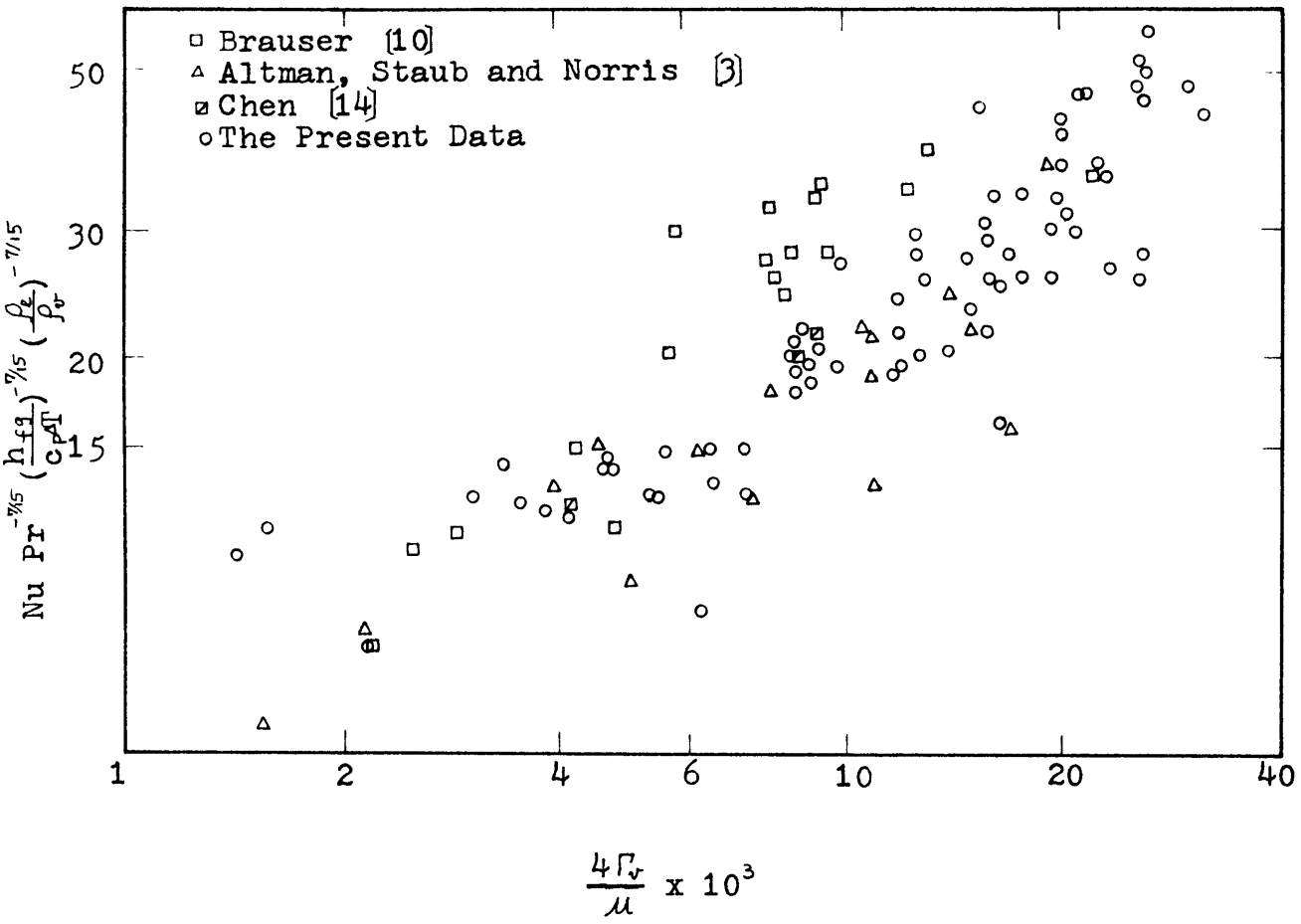

Fig. 7. Data on Brauser Plot

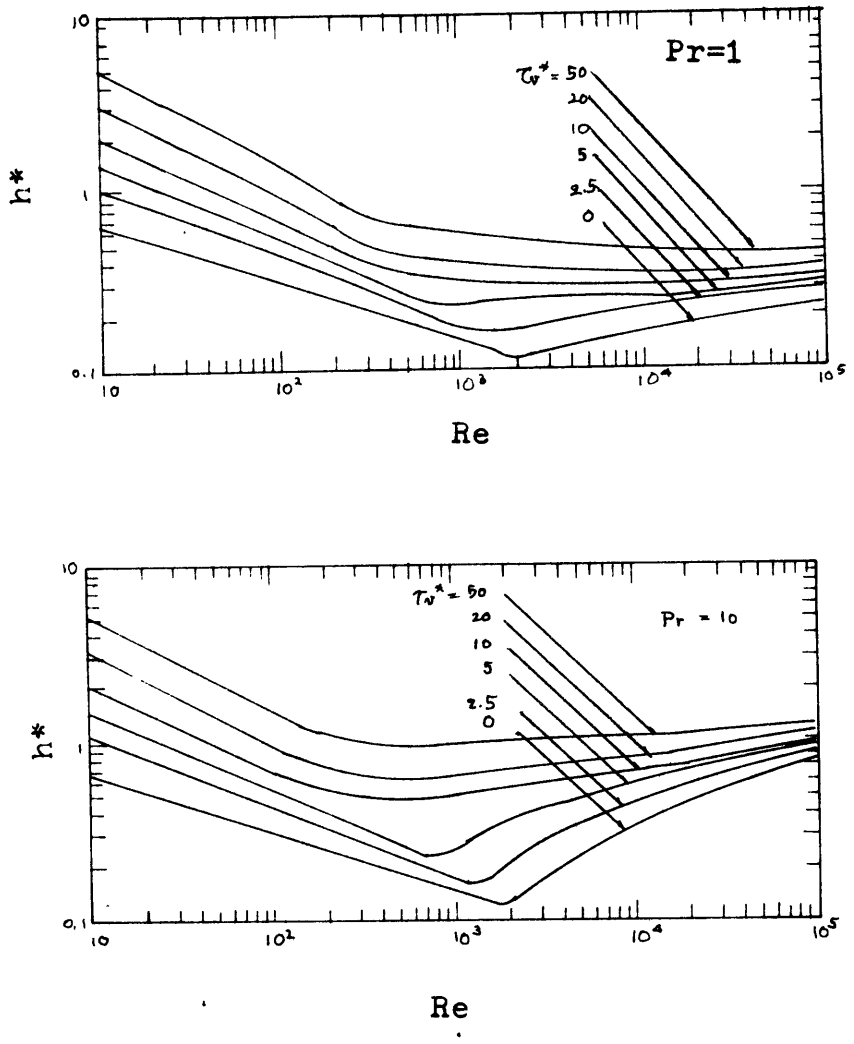

Fig. 8. Effect of Turbulence and Vapor Shear Stress on Condensation

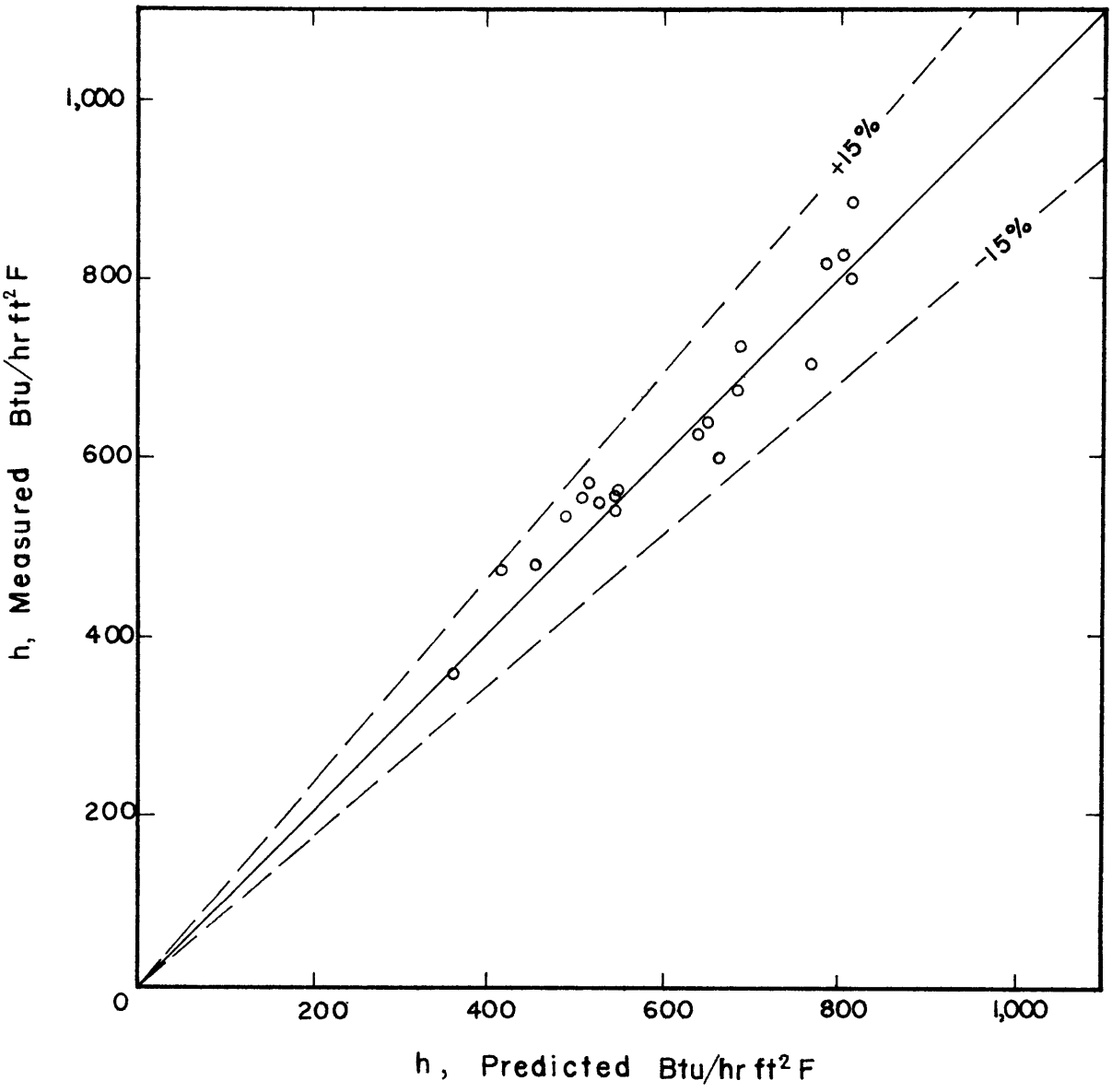

Fig. 9. Data Compared with Modified Rohsenow, Webber, and Ling Analysis

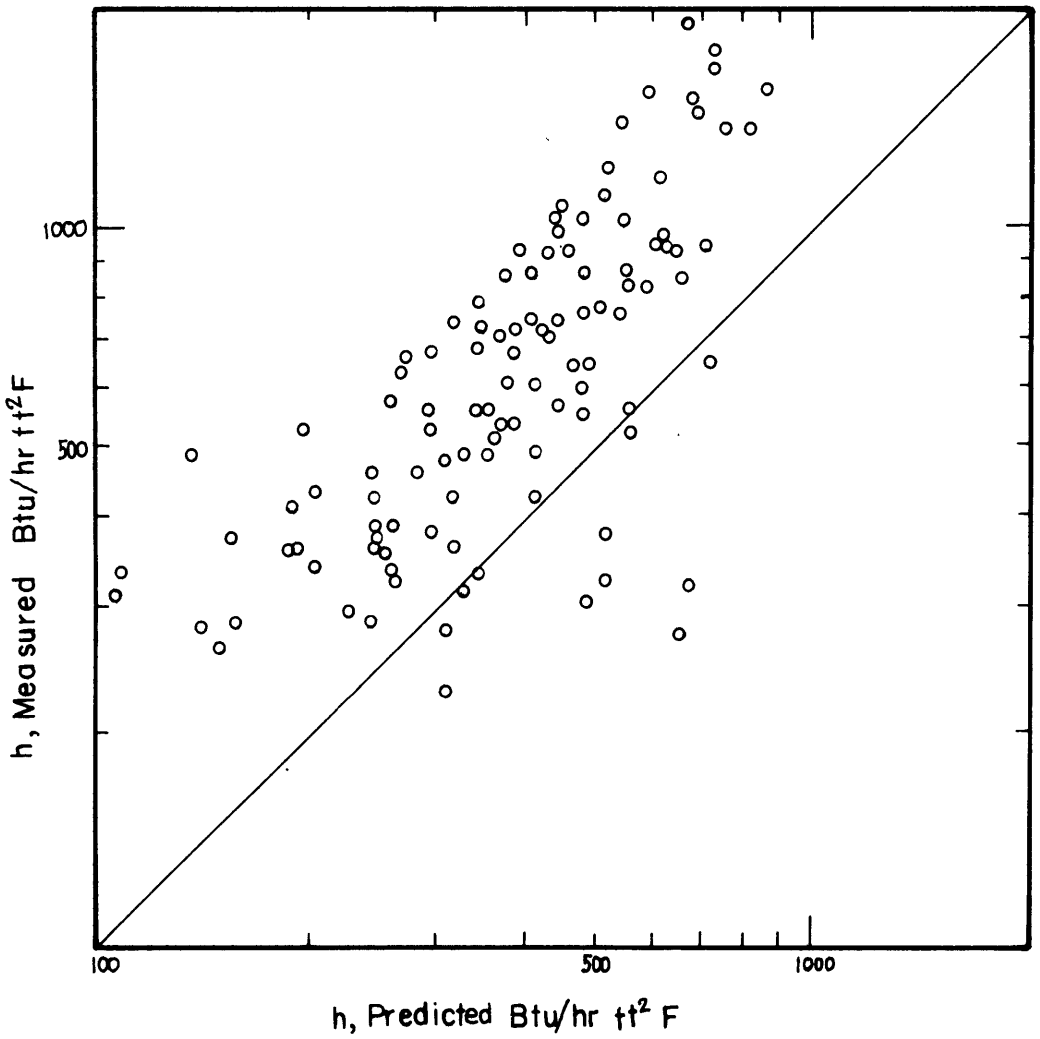

Fig. 10. Data Compared With Boyko-Kruzhilin Prediction.

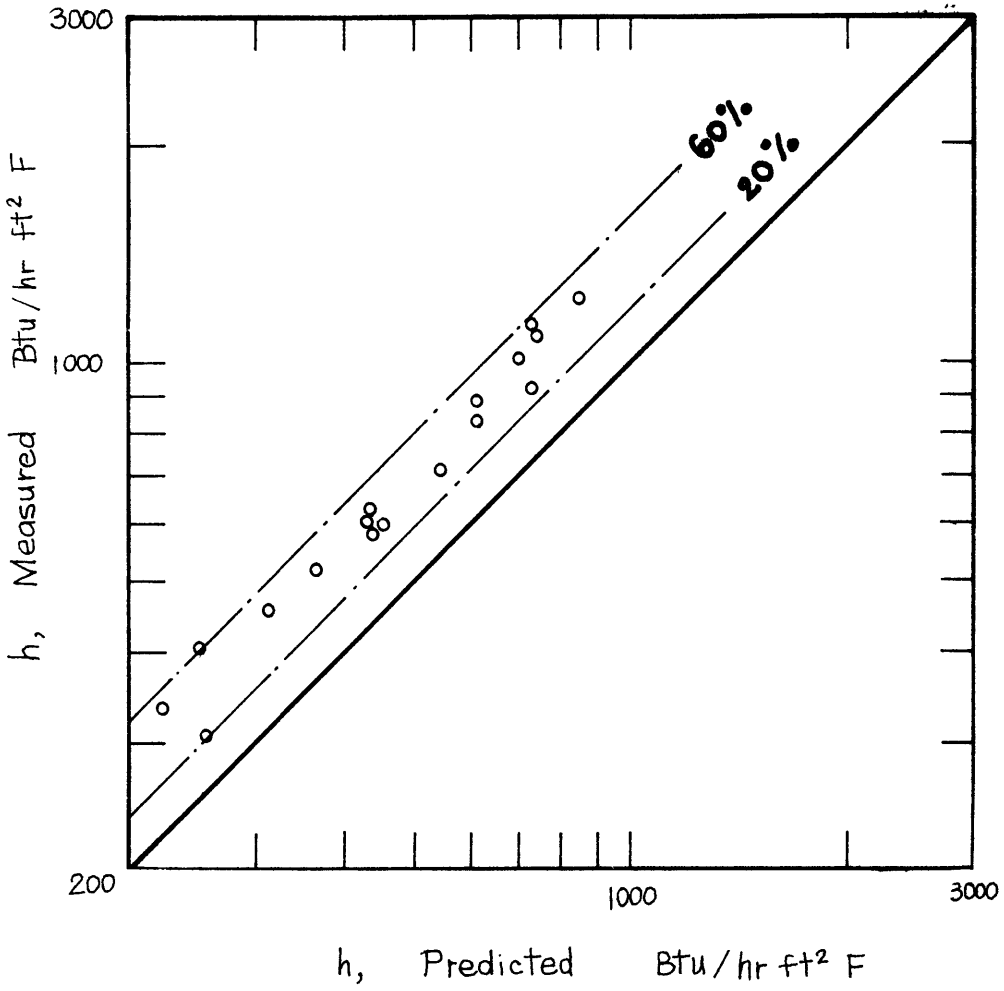

Figure 11. Altman et al [3] data compared with Boyko-Kruzhilin Prediction.